CENTER OF EXCELLENCE
WORKING PAPER SERIES

Nicole Branger - Patrick Grüning - Holger Kraft - Christoph Meinerding - Christian Schlag

Asset Pricing under Uncertainty about Shock Propagation

SAFE Working Paper Series No. 34

Center of Excellence SAFE Sustainable Architecture for Finance in Europe
A cooperation of the Center for Financial Studies and Goethe University Frankfurt

House of Finance | Goethe University
Grüneburgplatz 1 | D-60323 Frankfurt am Main

Tel. +49 (0)69 798 34006 | Fax +49 (0)69 798 33910
info@safe-frankfurt.de | www.safe-frankfurt.de

Non-Technical Summary

This paper deals with the equilibrium asset pricing implications of uncertainty about the propagation of economic crises from one sector of the economy to others. Such crises usually do not consist of just a single event, but instead unfold over time in a series of adverse shocks. Moreover, whether or not a shock to economic fundamentals marks the beginning of a longer-lasting economic downturn is typically unknown and can only be assessed better over time, i.e., there exists a large amount of uncertainty among market participants concerning the true state of the economy.

Although our model is not at all limited in its scope to extreme scenarios, two historical events can serve as nice examples for the basic intuition behind our approach. First, 'Black Friday' in October 1929 represented a large negative shock to the stock market, which triggered subsequent negative shocks to other sectors of the economy and marked the beginning of the Great Depression lasting for about a decade. Similarly, the Lehman default in September 2008 was in itself certainly a drastic event, but its negative impact became even stronger due to the fact that it spread through the whole economy and lead to the Great Recession, again an extended period of high volatility and pronounced economic uncertainty.

To provide a rationale for these patterns of drastic economy-wide crises we propose a model with two sectors and two economic states, one representing a 'crisis' or 'bad' state and the other one the 'normal' or 'good' state. A negative jump in the output of one sector can trigger an economy-wide crisis, but there are also 'normal' non-contagious shocks. The agent in our economy only observes the level of output, but not the underlying state, and thus cannot distinguish between the two types of jumps, so that the transmission of shocks is accompanied by a high degree of uncertainty. However, the investor can infer (noisy) information on the state from observing output, since we assume that the bad state is characterized by a much higher frequency of jumps and also a lower expected output growth.

While each of the key features of our model – multiple sectors, the propagation of shocks, and partial information about the economic state – has already been analyzed on its own in the asset pricing literature, we show that the interplay between them produces even richer results and can help explain a variety of asset pricing puzzles. In particular, we show that our crisis propagation mechanism produces countercyclical correlations of equity returns. Learning about whether shocks have transmitted across the economy leads to countercyclical return volatilities. Our model also matches the typical return and consumption growth predictability patterns in the data, i.e., returns are predictable by the price-dividend ratio whereas consumption growth is not. Furthermore, imperfect information about the state of the economy leads to a basically flat 'term structure of equity' in our model, meaning the term structure of expected returns on claims to single future dividend payments with different maturities. Having two heterogeneous sectors substantially

increases the persistence of price-dividend ratios. Finally, our model can match the equity premium with more moderate preference parameters than other jump-diffusion models.

To summarize, we provide evidence that incorporating realistic patterns of economic crises in a general equilibrium model can explain a large number of stylized facts of asset markets. Placing the model into an international context and thus studying the transmission of crises across countries (or continents) and the effect on exchange rates is a potentially interesting application of our setup and is left for further research.

Asset Pricing under Uncertainty about Shock Propagation

Nicole Branger* Patrick Grüning** Holger Kraft**
Christoph Meinerding** Christian Schlag**

This version: March 25, 2014

Abstract

We analyze the equilibrium in a two-tree (sector) economy with two regimes. The output of each tree is driven by a jump-diffusion process, and a downward jump in one sector of the economy can (but need not) trigger a shift to a regime where the likelihood of future jumps is generally higher. Furthermore, the true regime is unobservable, so that the representative Epstein-Zin investor has to extract the probability of being in a certain regime from the data. These two channels help us to match the stylized facts of countercyclical and excessive return volatilities and correlations between sectors. Moreover, the model reproduces the predictability of stock returns in the data without generating consumption growth predictability. The uncertainty about the state also reduces the slope of the term structure of equity. We document that heterogeneity between the two sectors with respect to shock propagation risk can lead to highly persistent aggregate price-dividend ratios. Finally, the possibility of jumps in one sector triggering higher overall jump probabilities boosts jump risk premia while uncertainty about the regime is the reason for sizeable diffusive risk premia.

Keywords: General Equilibrium, Contagion Risk, Partial Information, Filtering, Recursive Utility

JEL: G01, G12

*Finance Center Muenster, University of Muenster, Universitaetsstr. 14-16, 48143 Muenster, Germany. E-mail: nicole.branger@wiwi.uni-muenster.de.

**Department of Finance, Goethe-University, 60323 Frankfurt am Main, Germany. E-mails: patrick.gruening|holgerkraft|meinerding|schlag@finance.uni-frankfurt.de.

We thank seminar participants and colleagues at Goethe-University Frankfurt and the Wharton School for valuable comments and discussions. We gratefully acknowledge research and financial support from the Center of Excellence SAFE, funded by the State of Hessen initiative for research LOEWE. Holger Kraft gratefully acknowledges financial support by Deutsche Forschungsgemeinschaft (DFG).

"Fear is very contagious. You can get fearful in five minutes, but you don't get confident in five minutes."
Warren Buffett on CNBC, March 09, 2009

1 Introduction and Motivation

This paper deals with the equilibrium asset pricing implications of uncertainty about 'financial contagion' or, as we will mostly call it later, 'crisis propagation'. The mechanism through which shocks are transmitted from one sector of the economy to the other is one of the special features of our model with two sources for aggregate consumption ('two trees'). We distinguish between two types of (negative) shocks to the output of these trees: shocks of the first type only represent a downward jump in the cash flows of the respective tree, while shocks of the second type cause a regime switch to a state, where the likelihood of such large shocks is higher across all sectors. In this sense the crisis is propagated from one sector in the economy to the other. The transmission of shocks is, however, accompanied by a high degree of uncertainty, since the state of the economy is unobservable, i.e., the investor does not know whether there is currently a high or a low risk of such a jump event event triggering a large-scale and economy-wide crisis.

While each of these key features – multiple Lucas trees, partial information about the state, and the propagation of shocks – has already been analyzed on its own in the asset pricing literature, we show that the interplay between them produces even richer results and can help explain a variety of asset pricing puzzles. The equilibrium asset pricing dynamics in our model with two trees, two regimes, and learning go far beyond some sort of 'average' of different one-tree and one-regime economies. In particular, we show that our crisis propagation mechanism produces countercyclical correlations of equity returns. Learning about whether shocks have transmitted across the economy leads to countercyclical return volatilities. Our model also matches the typical return and consumption growth predictability patterns in the data. Furthermore, imperfect information about the state of the economy leads to a basically flat term structure of equity in our model, and having two heterogeneous trees substantially increases the persistence of price-dividend ratios. Finally, our model can match the equity premium with more moderate preference parameters than other jump-diffusion models.

Although our model is not at all limited in its scope to extreme scenarios, two historical events can serve as nice examples for the basic intuition behind our approach.

First, 'Black Friday' in October 1929 represented a large negative shock to the stock market, which triggered subsequent negative shocks to other sectors of the economy and marked the beginning of the Great Depression lasting for about a decade. Similarly, the Lehman default in September 2008 was in itself certainly a drastic event, but its negative impact became even stronger due to the fact that it spread through the whole economy and lead to the Great Recession, again an extended period of high volatility and a large amount of economic uncertainty. A key insight from the observation of these examples is thus that these contagion-like phenomena stretch out over a considerable amount of time. Furthermore, there is often one major event, which starts off a period of crisis with subsequent major shocks to markets other than the one affected initially.

So when we later on analyze crisis propagation from one sector of the economy to others in our model, we interpret this spreading of negative shocks as something with a time dimension, i.e., as something which unfolds over a series of events and a period of discrete length rather than it being represented by just one major shock which *simultaneously* affects several markets. At the same time, by the fact that such a period is characterized by multiple negative shocks, it is obvious that crisis propagation is closely connected to what is called 'tail risk', i.e., the risk of the occurrence of low probability, but high impact events.

Does the mechanism described in the above examples *automatically* imply that a pronounced shock to one sector of the economy always triggers a wide-reaching crisis? Not necessarily, as we argue, since it may well be that such a crash or large (negative) jump remains restricted to one part of the economy and does not cause the negative shocks to spread to other markets, i.e., it can be purely idiosyncratic. This in turn implies that we have to distinguish between the two types of jump-like shocks mentioned above, namely those which are 'contagious', i.e., which cause a regime shift, and those which do not.

The fact that there are these two types of jumps introduces the next modeling issue. If the agents in the economy could always exactly observe which of the two types of jumps has occurred, it would be a rather straightforward exercise to factor this into the computation of equilibrium asset prices and returns. However, it seems more realistic to assume that the state of the economy and thus the type of a jump is not observable. This fact is the motivation to include partial (or imperfect) information in our model in the sense that the investor has to filter the state ('contagious' or 'calm') from the observable data on output innovations. Our paper documents that, in a model with recursive preferences, the risk of future contagious jumps together with the imperfect observability of the state of the economy has first-order effects on asset prices, returns, volatilities, and

correlations.

Through the mechanism of crisis propagation from one sector to the next described above our model provides a rationale for the dynamics of economy-wide crises. Most importantly, the features of crisis propagation and incomplete information help us to match higher moments of asset returns in the data quite well. First, incomplete information about the state of the economy leads to excess volatility of risky asset returns, i.e., the volatility of equity returns is substantially higher than the volatilities of the associated consumption streams. Second, the fact that the degree of uncertainty is higher during crises than during normal 'calm' times makes the return volatilities countercyclical. Finally, the contagion feature in our model leads to countercyclical comovement between the sectors in the economy, i.e., the return correlation between the two sectors is higher when the economy is in a bad state, a stylized fact which has often been documented in the data[1] which can be considered common knowledge by now.[2]

A large literature[3] centers around the predictability of future stock returns given, e.g., the current price-dividend ratio. Many models, where future excess returns are actually predictable via the price-dividend ratio, simultaneously suffer from the problem that they also generate strong predictability of future dividend growth, which is not there in the data. Also here our model produces results which are almost perfectly in line with the empirical facts. Expected returns mostly depend on the current probability of jumps, while consumption growth rates are much more driven by the actual realization of these jumps. Consequently, equity returns are highly predictable in our model while consumptions growth rates are not.

Triggered by the work in Lettau and Wachter (2007) and van Binsbergen, Brandt, and Koijen (2012) some papers like Wachter (2013) and Belo, Collin-Dufresne, and Goldstein (2012) analyze the 'term structure of equity', meaning the term structure of expected returns on claims to single future dividend payments with different maturities. The claim put forward in van Binsbergen, Brandt, and Koijen (2012) is that this term structure is downward sloping in a rather pronounced fashion, although Boguth, Carlson, Fisher, and Simutin (2012) cast some doubt on this result. Overall our model does well with respect to this over-identifying restriction. The model-generated term structure does not exhibit a pronounced downward slope as in van Binsbergen, Brandt, and Koijen (2012) or Belo, Collin-Dufresne, and Goldstein (2012), but is flatter than the one in Wachter (2013),

[1] See, e.g., Longin and Solnik (2001) and Ehling and Heyerdahl-Larsen (2013).
[2] See, e.g., the article in the Wall Street Journal by Lauricella (2009).
[3] See, e.g., Bansal and Yaron (2004) and Cochrane (2008) as well as the references cited therein.

again a result due to the information structure in our economy.[4] It is also worth noting here that in contrast to Lettau and Wachter (2007) the pricing kernel in our model is not reverse-engineered to produce a certain term structure of equity, but is derived from fundamental assumptions about preferences and endowments.

Furthermore and important from a modeling perspective, we do not have to rely on the usual Peso problem story to explain the equity premium in the presence of jump risk. This feature of the model is highlighted by the fact that (in absolute values) much smaller jump sizes than usual are sufficient to match asset pricing moments, since it is the time dimension of the crisis propagation which mainly generates the results. In our model a jump size of -6% is sufficient to obtain sensible values for the equity premium and higher moments of stock returns, whereas models of the type initially proposed by Barro (2006, 2009) and then taken up by, e.g., Chen, Joslin, and Tran (2012) are built on the assumption of rare consumption disasters being of the order of -40%, a value which seems rather implausible given the history of the US economy, even when the Great Depression is included. Our model thus provides a possible solution to the critique by Constantinides (2008).

The fact that the investor cannot observe the state of the economy also generates sizeable *diffusive* risk premia, i.e., it is not just the jump part of consumption growth which makes the investor demand a compensation for risk. In this sense our model is more balanced and realistic than the aforementioned alternative approaches, since it seems quite reasonable to assume that investors are also concerned about 'normal' fluctuations in aggregate consumption and not just about rare events. Nevertheless, our model is also able to endogenously produce large jump risk premia due to the propagation feature, i.e., due to the fact that jumps in one asset can cause a switch to a regime with higher jump intensities overall.

Finally, in addition to the time series effects there are also cross-sectional implications of the risk of a crisis being propagated from one sector to the next. Our model with two trees allows us to study these effects within one given model economy, instead of having to compare differently parametrized versions of economies with only one tree. We observe that the two-tree framework has remarkable implications for the persistence of price-dividend ratios in the economy. The state variables in our model have relatively low autocorrelation which we need to get rid of the counterfactual consumption growth predictability. Nevertheless, the price-dividend ratios – in particular for small assets – are

[4]The empirical p-values in Belo, Collin-Dufresne, and Goldstein (2012) do not provide very strong evidence against a flat term structure.

highly persistent because of the interaction of the two-tree framework with the learning in the model. Moreover, the degree of persistence is even higher in an economy where the two trees are different in terms of their parametrization.

Our paper is related to several strands of the literature. First, it deals with a general equilibrium analysis of 'multiple-tree' economies, as discussed by, among others, Cochrane, Longstaff, and Santa-Clara (2008) and Martin (2013). Second, our paper is related to the recent debate about disaster risk and the equity premium puzzle pursued by Barro (2006, 2009), Constantinides (2008), Wachter (2013), Backus, Chernov, and Martin (2011), and Nakamura, Steinsson, Barro, and Ursúa (2013). The fact that some types of jumps have contagious effects links our paper to the literature on contagion, network effects, and propagation of shocks across markets, i.e., to papers like Branger, Kraft, and Meinerding (2013a), Ait-Sahalia, Cacho-Diaz, and Laeven (2013), Buraschi and Porchia (2012) and Benzoni, Collin-Dufresne, Goldstein, and Helwege (2011). The powerful element of incomplete information about the current state of the economy has been included in the models proposed by, among others, Veronesi (1999) or Brennan and Xia (2001). A detailed overview of this literature is provided by Pástor and Veronesi (2009), more recent papers with recursive preferences include Croce, Lettau, and Ludvigson (2012) and Collin-Dufresne, Johannes, and Lochstoer (2013). Finally, we employ recursive preferences, which can by now be considered (almost) standard in the asset pricing literature. This concept was introduced by Epstein and Zin (1989). The continuous-time case is discussed in detail in Duffie and Epstein (1992a,b) and applied in the context of a long-run risk model with jumps in Benzoni, Collin-Dufresne, and Goldstein (2011).

In the remainder of the paper we will first present the formal model in Section 2, followed by a derivation of the equilibrium in Section 3. Section 4 contains a detailed comparison between the model output and the data. Section 5 concludes the paper. All proofs and detailed discussions of the technical aspects of the model can be found in the appendix.

2 Model

2.1 Consumption Dynamics

We study a Lucas-type endowment economy, where aggregate consumption C is given as the sum of the outputs of two trees A and B, i.e., $C = C_A + C_B$.[5] Throughout the paper we will interpret the trees as two sectors of the economy. At any point in time the economy is in either of two states. Since our focus is on the pricing implications of the propagation of shocks, we denote the states by 'calm' and 'contagion' in the following. Since we will later assume that the state of the economy is unobservable, it is important to distinguish between the true model and the model as perceived by the representative investor who has to filter information about the unobservable state from the data.

Under the true model the consumption dynamics for the trees $i = A, B$ in the calm state are given by the following jump-diffusion process:

$$\frac{dC_{i,t}}{C_{i,t-}} = \mu_i^{calm} dt + \sigma_i dW_{i,t} + L_i d\tilde{N}_{i,t}^{calm,calm} + L_i d\tilde{N}_{i,t}^{calm,cont}, \tag{1}$$

whereas in the contagion state we have

$$\frac{dC_{i,t}}{C_{i,t-}} = \mu_i^{cont} dt + \sigma_i dW_{i,t} + L_i d\tilde{N}_{i,t}^{cont,cont}. \tag{2}$$

The parameters μ_i^j, σ_i, L_i, the intensities of the counting processes[6] $\tilde{N}_i^{j,k}$, and also the correlation ρ of the two Brownian motions W_A and W_B are constants. Note that the diffusive part of output growth is the same in the two states for both trees.

The first key assumption of our model is that shocks to the endowment processes can be propagated throughout the economy. As can be seen from Equation (1) there are two types of jump-driven shocks in the calm state. The processes $\tilde{N}_i^{calm,calm}$ collect 'normal' consumption shocks to the two trees, which occur rather infrequently and are of moderate size. In contrast the processes $\tilde{N}_i^{calm,cont}$ represent so-called 'contagious' shocks. Such shocks not only reduce C_A or C_B immediately, but also trigger a regime switch to the contagion state shown in Equation (2), which is characterized by high jump intensities for

[5] The fact that aggregate consumption is written as the sum of the output of the two trees implies that we treat C_A and C_B as perfect substitutes, as in Cochrane, Longstaff, and Santa-Clara (2008) and other papers in the literature on multiple-tree models. Perfect substitutability represents a special case of a general aggregation function with constant elasticity of substitution.

[6] The counting processes in our model are *not* Poisson processes, since the stopping times of different jump events are not mutually independent, as will become clear below.

the counting processes $N_i^{cont,cont}$. In particular we assume $\lambda_i^{cont,cont} \geq \lambda_i^{calm,calm} + \lambda_i^{calm,cont}$ for $i = A, B$. Finally, we assume that regime switches back from the contagion to the calm state (modeled by the counting process $\tilde{N}^{cont,calm}$ with intensity $\lambda^{cont,calm}$) do not affect any of the endowments directly.

Note that the drift rates μ_i^j are also allowed to depend on the state. They will in general be high in the calm state and low in the contagion state, reflecting the fact that we not only observe more frequent shocks in the contagion state, but also a lower overall growth rate of output.

The second key assumption of our model is that the state of the economy is unobservable. Before we describe the setup with incomplete information in detail below, we will first rewrite the output dynamics for the two trees in a more convenient fashion. Let the indicator variable p_t denote the state of the economy such that if $p_t = 1$, the economy is in the calm state, and in the contagion state otherwise. The consumption dynamics can then be reformulated as functions of p_t. Under the true model we have

$$\frac{dC_{i,t}}{C_{i,t-}} = \mu_{i,t}dt + \sigma_i dW_{i,t} + L_i dN_{i,t}^{calm,cont} + L_i dN_{i,t}^{calm,calm} + L_i dN_{i,t}^{cont,cont}, \tag{3}$$

and the state of the economy p_t has dynamics

$$dp_t = dN_t^{cont,calm} - (dN_{A,t}^{calm,cont} + dN_{B,t}^{calm,cont}). \tag{4}$$

The counting processes $N_i^{calm,calm}$, $N_i^{calm,cont}$, $N_i^{cont,cont}$, and $N^{cont,calm}$ introduced in (3) and (4) have intensities equal to $p_t\lambda_i^{calm,calm}$, $p_t\lambda_i^{calm,cont}$, $(1-p_t)\lambda_i^{cont,cont}$, and $(1-p_t)\lambda^{cont,calm}$, respectively, i.e., they are 'on' or 'off', depending on the state of the economy. The drift rates in (3) are given by $\mu_{i,t} \equiv p_t\mu_i^{calm} + (1-p_t)\mu_i^{cont}$.

As in Cochrane, Longstaff, and Santa-Clara (2008) and Martin (2013), we define the output share of tree A

$$s_{A,t} = \frac{C_{A,t}}{C_{A,t} + C_{B,t}}.$$

To make the notation more compact and easier to read we will from now on write $s_{B,t}$ instead of $1 - s_{A,t}$. With this the dynamics of aggregate consumption are given by

$$\begin{aligned}\frac{dC_t}{C_{t-}} = &\left[s_{A,t}\mu_{A,t} + s_{B,t}\mu_{B,t}\right]dt + s_{A,t}\sigma_A dW_{A,t} + s_{B,t}\sigma_B dW_{B,t} \\ &+ s_{A,t-}L_A\left(dN_{A,t}^{calm,calm} + dN_{A,t}^{calm,cont} + dN_{A,t}^{cont,cont}\right)\end{aligned}$$

$$+ s_{B,t-} L_B \left(dN_{B,t}^{calm,calm} + dN_{B,t}^{calm,cont} + dN_{B,t}^{cont,cont} \right).$$

An application of Itô's Lemma leads to the normalized output share dynamics

$$\begin{aligned}
\frac{ds_{A,t}}{s_{A,t-} s_{B,t-}} = & \left[\mu_{A,t} - \mu_{B,t} - s_{A,t}\sigma_A^2 + s_{B,t}\sigma_B^2 + (s_{A,t} - s_{B,t})\rho\sigma_A\sigma_B \right] dt + \sigma_A dW_{A,t} - \sigma_B dW_{B,t} \\
& + \frac{L_A}{1 + L_A s_{A,t-}} \left(dN_{A,t}^{calm,calm} + dN_{A,t}^{calm,cont} + dN_{A,t}^{cont,cont} \right) \\
& - \frac{L_B}{1 + L_B s_{B,t-}} \left(dN_{B,t}^{calm,calm} + dN_{B,t}^{calm,cont} + dN_{B,t}^{cont,cont} \right).
\end{aligned}$$

The interpretation here is straightforward. Downward jumps in the output of tree A reduce its output share, whereas downward jumps in tree B increase it. In order to further simplify notation, we denote the output share of tree A after a jump in tree A by $s_{A,t}^{A+} \equiv s_{A,t-} \frac{1+L_A}{1+L_A s_{A,t-}}$. Analogously, after a jump in tree B, $s_{A,t}^{B+} \equiv s_{A,t-} \frac{1}{1+L_B(1-s_{A,t-})}$.

2.2 Representative Agent

The representative agent has recursive preferences over aggregate consumption. Following Duffie and Epstein (1992b), we define the indirect utility function as

$$J_t = E_t \left[\int_t^\infty f(C_s, J_s) ds \right],$$

with the aggregator function

$$f(C, J) = \frac{\beta C^{1-\frac{1}{\psi}}}{\left(1 - \frac{1}{\psi}\right) \left[(1-\gamma)J\right]^{\frac{1}{\theta}-1}} - \beta\theta J.$$

The relative risk aversion, the elasticity of intertemporal substitution, and the subjective time discount factor are denoted by γ, ψ, and β, respectively. We assume that the agent has a preference for early resolution of uncertainty, i.e., we assume $\theta \equiv \frac{1-\gamma}{1-\frac{1}{\psi}} < 1$.

2.3 Learning

As stated above a key assumption of our model is that the state of the economy p_t is unobservable. The agent can only observe the output streams $C_{A,t}$ and $C_{B,t}$, but not the true p_t. Technically, this means that the agent has to base her decisions on a filtration

$\mathcal{G} \subseteq \mathcal{F}$, where $\mathcal{F}$ is the filtration associated with the full information case. Since they are observable, the processes C_A and C_B are adapted to the filtration $\mathcal{G}$, but the state variable p is not.

The agent's decisions (and thus all equilibrium asset pricing results) depend on the filtered estimate for p_t, denoted by $\widehat{p}_t$, which is the conditional expectation of p_t, given the investor's information at time t, i.e., $\widehat{p}_t = E[p_t|\mathcal{G}_t]$. The dynamics of $\widehat{p}$ are stated in

Proposition 1. *The filtered probability $\widehat{p}_t$ follows the process*

$$\begin{aligned} d\widehat{p}_t &= \left((1-\widehat{p}_t)\lambda^{cont,calm} - \widehat{p}_t(\lambda_A^{calm,cont} + \lambda_B^{calm,cont})\right) dt \\ &\quad + \widehat{p}_t(1-\widehat{p}_t) \begin{pmatrix} \mu_A^{calm} - \mu_A^{cont} \\ \mu_B^{calm} - \mu_B^{cont} \end{pmatrix}^T \left(\Sigma\Sigma^T\right)^{-1} \Sigma_{AB} \begin{pmatrix} d\widehat{W}_{A,t} \\ d\widehat{W}_{B,t} \end{pmatrix} \\ &\quad + \sum_{i=A,B} \widehat{p}_{t-} \left(\frac{\lambda_i^{calm,calm}}{\widehat{\lambda}_{i,t}} - 1\right) \left(d\widehat{N}_{i,t} - \widehat{\lambda}_{i,t}dt\right) \end{aligned} \tag{5}$$

with

$$\Sigma_{AB} = \begin{pmatrix} \sigma_A & 0 \\ 0 & \sigma_B \end{pmatrix} \qquad \textit{and} \qquad \Sigma = \begin{pmatrix} \sigma_A & 0 \\ \rho\sigma_B & \sqrt{1-\rho^2}\sigma_B \end{pmatrix}.$$

A short proof along the lines of Branger, Kraft, and Meinerding (2013b) is given in Appendix A.1. In (5) $\widehat{W}_i$ and $\widehat{N}_i$ denote the Brownian motions and jump process as perceived by the investor. They are related to the true processes via

$$\begin{aligned} d\widehat{N}_{i,t} &= dN_{i,t}^{calm,calm} + dN_{i,t}^{calm,cont} + dN_{i,t}^{cont,cont} \\ d\widehat{W}_{i,t} &= dW_{i,t} + \sigma_i^{-1}(\mu_{i,t} - \widehat{\mu}_{i,t})dt. \end{aligned} \tag{6}$$

The filtered drift rates and the jump intensities for $\widehat{N}_i$ are given by

$$\begin{aligned} \widehat{\mu}_{i,t} &= \widehat{p}_t\mu_i^{calm} + (1-\widehat{p}_t)\mu_i^{cont} \\ \widehat{\lambda}_{i,t} &= \widehat{p}_t\left(\lambda_i^{calm,calm} + \lambda_i^{calm,cont}\right) + (1-\widehat{p}_t)\lambda_i^{cont,cont}. \end{aligned}$$

Finally the dynamics of the two consumption streams under the investor's filtration are

$$\frac{dC_{i,t}}{C_{i,t-}} = \widehat{\mu}_{i,t}dt + \sigma_i d\widehat{W}_{i,t} + L_i d\widehat{N}_{i,t} \qquad (i = A, B).$$

Since our model is formulated in continuous time, the investor can perfectly distinguish between diffusive noise and jumps. However, she cannot distinguish between different

types of jumps, i.e., she cannot identify whether a jump in one of the trees has been contagious or normal. A shock in one of the trees, no matter of which type, thus always reduces the estimated probability $\widehat{p}_t$ of being in the calm state. This can be seen from the last term (the sum) in (5), since by assumption $\lambda_i^{cont,cont} \geq \lambda_i^{calm,calm} + \lambda_i^{calm,cont}$, so that $\widehat{\lambda}_{i,t} \geq \lambda_i^{calm,calm} + \lambda_i^{calm,cont} \geq \lambda_i^{calm,calm}$, which makes the second factor in the product after the summation sign negative. In analogy to our short hand notation for the output shares after jumps in C_A or C_B we compactly write $\widehat{p}_t^{A+} \equiv \widehat{p}_{t-} \frac{\lambda_A^{calm,calm}}{\widehat{\lambda}_{A,t-}}$ and $\widehat{p}_t^{B+} \equiv \widehat{p}_{t-} \frac{\lambda_B^{calm,calm}}{\widehat{\lambda}_{B,t-}}$ for the value of $\widehat{p}_t$ after a jump in C_A or C_B, respectively. Moreover, the estimate for p_t is continuously updated due to diffusive information, since in general the drift rates μ_i^j in the two states will differ.

In order to provide some intuition for the properties of the endowment processes and the filtering equation, Figure 1 shows simulation paths for C_A, C_B, p, and $\widehat{p}$ based on the parameters in the column labeled 'Benchmark' in Table 1 and the filtering equation (5). The first contagion period starting around day 750 (indicated by the true state p being equal to zero) is triggered by a downward jump in C_A (blue line), the second one around day 3250 by a jump in C_B. We can nicely see the mechanics of filtering at work here, when the probability estimate $\widehat{p}_t$ also reacts to normal jumps with a substantial downward change. However, it reverts upwards rather quickly once a jump turns out to have been non-contagious. Between jumps, filtering from diffusion generates additional noise in $\widehat{p}_t$. The lower graph shows that the prices of the claims to the output of trees A an B exactly mirror the dynamics of $\widehat{p}$, especially at times of (truly) normal shocks, which nevertheless lead to a higher *estimated* probability of being in the contagious state and thus lower asset prices.

The filtered dynamics under $\mathcal{G}$ of aggregate consumption and the normalized output share of tree A are given by

$$\begin{aligned}\frac{dC_t}{C_{t-}} &= \left[s_{A,t}\widehat{\mu}_{A,t} + s_{B,t}\widehat{\mu}_{B,t}\right] dt + s_{A,t}\sigma_A d\widehat{W}_{A,t} + s_{B,t}\sigma_B d\widehat{W}_{B,t} \\ &\quad + s_{A,t-}L_A d\widehat{N}_{A,t} + s_{B,t-}L_B d\widehat{N}_{B,t}, \end{aligned} \tag{7}$$

and

$$\begin{aligned}\frac{ds_{A,t}}{s_{A,t-}s_{B,t-}} &= \left[\widehat{\mu}_{A,t} - \widehat{\mu}_{B,t} - s_{A,t}\sigma_A^2 + s_{B,t}\sigma_B^2 + (s_{A,t} - s_{B,t})\rho\sigma_A\sigma_B\right] dt \\ &\quad + \sigma_A d\widehat{W}_{A,t} - \sigma_B d\widehat{W}_{B,t} + \frac{L_A}{1 + L_A s_{A,t-}} d\widehat{N}_{A,t} - \frac{L_B}{1 + L_B s_{B,t-}} d\widehat{N}_{B,t}.\end{aligned}$$

Since the process s_A involves the same Wiener processes and jump processes as C_A and C_B it cannot provide any news about the state of the economy, and its innovations are informationally redundant.

Besides the two endowment processes, we will also analyze two equity claims which we define as claims to levered consumption with cash flows $D_i = C_i^\phi$ $(i = A, B)$ where $\phi > 1$.[7] We call these claims asset A and B in the following. Under the true model Itô's Lemma implies the dynamics

$$\begin{aligned}\frac{dD_{i,t}}{D_{i,t-}} = &\left(\phi\mu_{i,t} + \frac{1}{2}\phi(\phi-1)\sigma_i^2\right)dt + \phi\sigma_i dW_{i,t} + ((1+L_i)^\phi - 1)dN_{i,t}^{calm,calm} \\ &+ ((1+L_i)^\phi - 1)dN_{i,t}^{calm,cont} + ((1+L_i)^\phi - 1)dN_{i,t}^{cont,cont}.\end{aligned}$$

whereas from the investor's perspective

$$\frac{dD_{i,t}}{D_{i,t-}} = \left(\phi\widehat{\mu}_{i,t} + \frac{1}{2}\phi(\phi-1)\sigma_i^2\right)dt + \phi\sigma_i d\widehat{W}_{i,t} + ((1+L_i)^\phi - 1)d\widehat{N}_{i,t}.$$

3 Equilibrium

According to Duffie and Epstein (1992a), the representative investor's pricing kernel ξ is given by

$$\xi_t = \beta^\theta C_t^{-\gamma} e^{-\beta\theta t + (\theta-1)\left(\int_0^t e^{-v_u}du + v_t\right)}, \tag{8}$$

where v_t is the logarithm of the wealth-consumption ratio. So in order to price assets in this economy, we first need to determine the equilibrium wealth-consumption ratio. $v_t = v\left(s_A, \widehat{p}\right)$ depends on two state variables, the output share s_A and the filtered probability of being in the calm state $\widehat{p}$. [8] To solve for v_t, we apply the Bellman equation from Duffie and Epstein (1992a):

$$0 = f(C_t, J_t) + \mathcal{D}J_t,$$

with $\mathcal{D}$ representing the usual differential operator, defined in Appendix A.2. With the usual conjecture

$$J = \frac{C^{1-\gamma}}{1-\gamma}\beta^\theta e^{\theta v},$$

[7] Note that some care has to be taken when introducing new assets into the model, since if these assets provide a non-redundant signal about the state of the economy the filtering problem of the agent would be different from the start. In order to avoid these issues we work with the levered dividends.

[8] For the sake of readability, we omit the time index of s_A and $\widehat{p}$ in the following.

we can then deduce the following partial differential equation for v.

Proposition 2. *The log wealth-consumption ratio v solves the following partial differential equation:*

$$\begin{aligned} 0 \;=\; & e^{-v(s_A,\widehat{p})} - \beta + \left(1-\frac{1}{\psi}\right)\mu_C - \frac{1}{2}\gamma\left(1-\frac{1}{\psi}\right)\sigma_{CC} + v_s\mu_s + \frac{1}{2}\left(v_{ss}+\theta(v_s)^2\right)\sigma_{ss} \\ & + v_{\widehat{p}}\mu_{\widehat{p}} + \frac{1}{2}\left(v_{\widehat{p}\widehat{p}}+\theta(v_{\widehat{p}})^2\right)\sigma_{\widehat{p}\widehat{p}} + (1-\gamma)v_s\sigma_{Cs} + (1-\gamma)v_{\widehat{p}}\sigma_{C\widehat{p}} + \left(v_{s\widehat{p}}+\theta v_s v_{\widehat{p}}\right)\sigma_{s\widehat{p}} \\ & + \frac{1}{\theta}\widehat{\lambda}_A\left[(1+s_AL_A)^{1-\gamma}e^{\theta v(s_A^{A+},\widehat{p}^{A+})-\theta v(s_A,\widehat{p})}-1\right] \\ & + \frac{1}{\theta}\widehat{\lambda}_B\left[(1+s_BL_B)^{1-\gamma}e^{\theta v(s_A^{B+},\widehat{p}^{B+})-\theta v(s_A,\widehat{p})}-1\right], \end{aligned}$$

where μ_C, σ_{CC}, μ_s, σ_{ss}, $\mu_{\widehat{p}}$, $\sigma_{\widehat{p}\widehat{p}}$, σ_{Cs}, $\sigma_{C\widehat{p}}$ and $\sigma_{s\widehat{p}}$ are defined in Appendix A.2.

A detailed proof is given in Appendix A.2, where we also discuss the numerical solution of this PDE in detail.

We can use the pricing kernel from (8) to price other assets in the economy. Here, we will focus on the two equity claims with dividend flow (as perceived by the investor)

$$\frac{dD_{i,t}}{D_{i,t-}} = \left(\phi\widehat{\mu}_{i,t} + \frac{1}{2}\phi(\phi-1)\sigma_i^2\right)dt + \phi\sigma_i d\widehat{W}_{i,t} + ((1+L_i)^\phi - 1)d\widehat{N}_{i,t}.$$

A Feynman-Kac argument, which is presented in detail in Appendix A.3, leads to partial differential equations for the log price-dividend ratio of assets A and B, ω_A and ω_B, as functions of s_A and $\widehat{p}$. These partial differential equations are structurally very similar to those for the log wealth-consumption ratio v in Proposition 2, so that we can apply the solution techniques for the latter also here.

4 Comparing the Model to the Data

4.1 Benchmark Calibration

In order to derive quantitative implications we assume the parameter values reported in the first column of Table 1. The preference parameters $\gamma = 10$ and $\psi = 2$ are in line with the long-run risk literature, see, e.g., Bansal and Yaron (2004). All other parameters are chosen to match aggregate US data.

Since macroeconomic data is available at most on a quarterly basis, it is hard to calibrate a jump-diffusion model to consumption data. This is especially true for our paper, since we do not suggest a typical Peso problem story from disaster models like Barro (2006, 2009). Instead, we choose higher jump frequencies, but more moderate jump sizes in the spirit of Backus, Chernov, and Martin (2011), who try to match option data and macroeconomic data, or Constantinides (2008). Each type of shock in the calm state has an intensity of 0.125 and a size of -0.06. If both trees are equally large, i.e. $s_A = 0.5$, this implies on average one consumption shock of -0.03 every other year. In the contagion state, the intensity of consumption shocks is increased to 0.8 in both trees. The diffusion parameters for output growth σ_i are set to a moderate level of 0.01, and we assume a diffusion correlation $\rho = 0$ for simplicity.[9] Together with the drift rates $\mu_i^{calm} = 0.047$ and $\mu_i^{cont} = 0.019$, our choices imply an unconditional annual expected growth rate of consumption of 1.9 percent. The contagion state in our model is assumed to have an average duration of 1 year, i.e. $\lambda^{cont,calm} = 1$. The unconditional probabilities of the two economic states are roughly in line with the time the US economy has spent in NBER recessions since 1947, which is around 20%.

Finally, the leverage parameter $\phi = 2.5$ and the subjective discount rate $\beta = 0.039$ are chosen such that the equity premium and the risk-free rate in the data can be matched and the price-dividend ratios in the model remain finite.

A natural question arising in a model with two trees is about the economic interpretation of the two endowment processes. In the calibration above, we implicitly assume that our economy consists of two more or less identical sectors. When the two sectors have equally large outputs, the sum of these outputs then has dynamics which are similar to consumption dynamics in the data. However, we can also study the equilibrium with sectors of different sizes. This is very useful, since, as documented by Cochrane, Longstaff, and Santa-Clara (2008) and Martin (2013), the spillover effects and the propagation of shocks depend on the relative size of the trees. In addition to this the interpretation of the trees as different sectors also gives rise to deeper cross-sectional analyses. We will therefore also analyze calibrations of the model in which the output processes of the two trees have different parameters. The calibrations are presented in the remaining columns of Table 1.

[9] In addition to being simpler computationally the assumption of $\rho = 0$ makes any correlation between the prices of trees an endogenous result generated only by the equilibrium pricing mechanism.

4.2 Simulating the Model

We use the numerical solutions for the wealth-consumption and price-dividend ratios to compute model-implied moments of asset returns as functions of s_A and $\widehat{p}$. Such an analysis helps to understand the mechanics of our model, but it does not tell us how well our model can match actual data. Therefore, we also perform Monte Carlo simulations of our model. We simulate the two trees on a daily frequency and draw 10,000 random paths each with a length of 65 years. For simplicity, we set the starting value of s_A and p equal to 0.5 and 1, respectively.[10] We then use the model-implied wealth-consumption and price-dividend ratios to compute time series of prices and returns for all assets, from which we then compute the statistics reported in the first column of Table 2.

Concerning our model setup one comment is necessary at this point. We are aware of the fact that the state variable s_A in our model is nonstationary so that, strictly speaking, one cannot analyze the model in the steady state. However, to the best of our knowledge, there are not many tractable alternative ways of modeling Lucas orchard economies which would ensure a non-degenerate stationary distribution of the output share.[11] In our model simulations we focus on a time horizon of 65 years, since this seems comparable to most of the data samples used in the asset pricing literature to date and the nonstationarity should not matter too much over this period length. Moreover, we have performed robustness checks where we extended the time window of the simulation to 500 years. Indeed, the output share s_A tends to 0 or 1 in the very long run. However, only for about 3% of all simulated paths we observe an output share below 0.2 or above 0.8 after 500 years, and of course this percentage is even smaller for more extreme values of s_A. The nonstationarity thus only matters for extremely long horizons, and we claim that the quantities generated by our model can be compared meaningfully to the data. Moreover, we will discuss the influence of the output share s_A on the asset pricing results in more detail in Section 4.9.

Table 2 reports the annual means, standard deviations and first-order autocorrelations for the fundamental cash flows and for a number of asset pricing quantities for the data and for our model. In terms of model-generated moments the return correlation $corr(r_A, r_B)$ has been computed from monthly returns over a rolling window of four years. The numbers referring to the aggregate dividend growth and the price-dividend ratio of

[10] The economy is thus initially assumed to be in the calm state. Choosing $p = 0$ as the initial value instead does not affect any of our results, since regime changes are relatively frequent in our model.

[11] See the discussion of this matter in an earlier working paper version of Cochrane, Longstaff, and Santa-Clara (2008) or in Menzly, Santos, and Veronesi (2004).

the market give the moments of the claim to aggregate dividends $D = D_A + D_B$.

The values in the columns labeled 'Data' are from a number of papers, but mostly from Benzoni, Collin-Dufresne, and Goldstein (2011), who use U.S. data from 1946 to 2008. The moments for the risk-free rate refer to the 3-month T-bill rate as reported by Wachter (2013). The statistics on correlations and sectoral dividends are taken from Ehling and Heyerdahl-Larsen (2013) and, finally, details about the wealth-consumption ratio and several autocorrelations are taken from either Lustig, van Nieuwerburgh, and Verdelhan (2013) or Bansal, Kiku, Shaliastovich, and Yaron (2013).

Mean consumption growth is 0.019 as calibrated and consumption growth volatility is 0.028. These numbers are well in line with the data. In particular, the dataset used in Barro (2006, 2009) shows that consumption volatilities are low only in subsamples without realizations of disasters (like the US after World War II). Instead, we try to explain asset pricing moments with more moderate, but at the same time more frequent consumption shocks and include these jumps in our samples. The properties of the model with respect to the volatility of aggregate dividend growth are similar to those for consumption. It is slightly higher than in the data and also more volatile, but nearly as persistent. However, our model results are generated including all consumption and dividend shocks in the sample. For the dividend growth rates of the individual trees, there is no clear empirical counterpart. Recently, Ehling and Heyerdahl-Larsen (2013) have estimated a standard deviation of dividends on the industry level of 0.133. Regarding our trees as representing different sectors of the economy, our model results look consistent with such evidence.

The level of the price-to-fundamentals ratios in our model is roughly in line with the data. Lustig, van Nieuwerburgh, and Verdelhan (2013), e.g., report a log wealth-consumption ratio of 4.63 using data from 1952 to 2011, so that the model is a little bit on the low side here. The level of the price-dividend ratio is matched much more closely. Furthermore, both the wealth-consumption ratio and the price-dividend ratios are also quite persistent in our model, with autocorrelations up to 0.74. The volatility of price-to-cashflow ratios is again somewhat low in the model, for which a look at Figure 2 provides an explanation. The state variable $\widehat{p}$ is much more volatile than the state variable s_A. However, the price-to-fundamentals ratios react to s_A much more than to $\widehat{p}$. A more detailed discussion of the properties of the price-to-fundamentals ratios can be found in Appendix B.

4.3 Risk-free Rate

The risk-free rate is obtained as the negative of the drift of the pricing kernel:

Proposition 3. *The risk-free rate is given by*

$$\begin{aligned} r_f = \beta &+ \frac{1}{\psi}\mu_C - \frac{1}{2}\gamma\left(1+\frac{1}{\psi}\right)\sigma_{CC} - (1-\theta)v_s\sigma_{Cs} - (1-\theta)v_{\widehat{p}}\sigma_{C\widehat{p}} \\ &- \frac{1}{2}(1-\theta)v_s^2\sigma_{ss} - \frac{1}{2}(1-\theta)v_{\widehat{p}}^2\sigma_{\widehat{p}\widehat{p}} - (1-\theta)v_s v_{\widehat{p}}\sigma_{s\widehat{p}} \\ &- \widehat{\lambda}_A\left[\eta_A^{jump} + \frac{1-\theta}{\theta}\left((1+s_AL_A)^{1-\gamma}e^{\theta\left(v(s_A^{A+},\widehat{p}^{A+})-v(s_A,\widehat{p})\right)}-1\right)\right] \\ &- \widehat{\lambda}_B\left[\eta_B^{jump} + \frac{1-\theta}{\theta}\left((1+s_BL_B)^{1-\gamma}e^{\theta\left(v(s_A^{B+},\widehat{p}^{B+})-v(s_A,\widehat{p})\right)}-1\right)\right]. \end{aligned}$$

For a proof see Appendix A.4.

The risk-free rate in our model comprises the typical terms: the time preference rate β, the expected growth rate of consumption scaled by the elasticity of intertemporal substitution, and a bunch of precautionary savings terms which lower the rate and thus help to resolve the risk-free rate puzzle.

The upper right graph of Figure 2 depicts the risk-free short rate in $[s_A, \widehat{p}]$-space. First of all, the risk-free rate is symmetric and concave in s_A. The aggregate consumption risk is the smallest at $s_A = 0.5$ and so are (the absolute values of) the corresponding precautionary savings terms. This diversification effect is especially pronounced for jumps. If s_A is close to 0 or 1, aggregate consumption can drop by either 6% or 0% (depending on which tree exhibits the shock). This risk is perceived far worse by the investor than the risk of twice as many medium-sized consumption drops if s_A is around 0.5. The dependence of the risk-free rate on the state variable $\widehat{p}$ basically mirrors the expected consumption growth rate. The interest rate is about 3.1 to 3.8 percentage points smaller for $\widehat{p} = 0$ than for $\widehat{p} = 1$. The convexity is again a result of the uncertainty about the state which has an additional effect through the precautionary savings terms.

The simulation results in Table 2 show that the standard deviation of the risk-free rate is about 0.0129, which seems to be in line with US data. The average level of the risk-free short rate in the simulations is 0.0352 since most of the time $\widehat{p}$ is close to 1. Depending on which data sample is used, these numbers seems to be in a plausible range.

4.4 Market Prices of Risk and Risk Premia

The risk premia of all assets follow from the market prices of risk in the economy and the exposures of the asset prices to the respective risk factors. Appendix A.4 states the dynamics of the pricing kernel, assuming a solution for the log wealth-consumption ratio v. From these we can directly determine the market prices of risk.

Proposition 4. *The market prices of diffusive risk are*

$$\eta_A^{diff} = \gamma s_A \sigma_A - (\theta-1) v_s s_A s_B \sigma_A - (\theta-1) v_{\widehat{p}} \widehat{p}(1-\widehat{p}) \left(\frac{(\mu_A^{calm} - \mu_A^{cont})}{(1-\rho^2)\sigma_A} - \frac{\rho(\mu_B^{calm} - \mu_B^{cont})}{(1-\rho^2)\sigma_B} \right)$$

$$\eta_B^{diff} = \gamma s_B \sigma_B + (\theta-1) v_s s_A s_B \sigma_B - (\theta-1) v_{\widehat{p}} \widehat{p}(1-\widehat{p}) \left(\frac{(\mu_B^{calm} - \mu_B^{cont})}{(1-\rho^2)\sigma_B} - \frac{\rho(\mu_A^{calm} - \mu_A^{cont})}{(1-\rho^2)\sigma_A} \right).$$

The market prices of jump risk are

$$\eta_i^{jump} = (1 + s_i L_i)^{-\gamma} e^{(\theta-1)\left(v(s_A^{i+}, \widehat{p}^{i+}) - v(s_A, \widehat{p})\right)} - 1,$$

where $i \in \{A, B\}$. The jump intensities under the risk-neutral measure, $\widehat{\lambda}_i^{\mathbb{Q}}$, equal the physical intensities $\widehat{\lambda}_i$, multiplied by $1+\eta_i^{jump}$. The market price of risk for the (unobservable) regime switches from the contagion state to the calm state is zero.

The market price of diffusion risk of tree A is depicted in the upper left graph of Figure 3. Analytically, the proposition shows that the market price of diffusive risk of tree i comprises three terms. The (standard) first term reflects the contribution of tree i to aggregate diffusive consumption risk. The second and third term represent the compensation for shocks to the state variables s_A and $\widehat{p}$, respectively. Since the representative agent has a preference for the early resolution of uncertainty, she not only cares about the local distribution of consumption, i.e., about 'immediate' consumption risk, but also about the fact that the continuation value of her indirect utility depends on state variables and is hence stochastic. In a world with CRRA preferences where $\theta = 1$, the corresponding market prices of state variable risk would be zero. A decomposition of the numerical results (not shown here) reveals that the market price of s_A-risk is relatively small. The third term however is numerically large for $\widehat{p}$ close to 0.5. Compared to an economy with full information, the additional amount of uncertainty dramatically increases the diffusion risk in the economy and leads to overall high market prices of diffusive risk, especially for intermediate values of $\widehat{p}$.

The upper right graph of Figure 3 depicts the market price of jump risk of tree A.

The fact that there is only one market price of jump risk despite there being three different counting processes driving the output of tree i is of course due to the assumption of partial information. The investor cannot distinguish between the different types of shocks and therefore applies the same market price to all of them. Moreover, the market price of risk for pure regime switches, which do not impact output, is equal to zero when the state of the economy is latent and unobservable. Therefore, the risk of transitions from the contagion state back to the calm state does not induce a premium in our model.

Analytically, the market price of jump risk in tree i is a product of two factors. The first factor, which is numerically larger, is the compensation for the immediate impact of jumps on the consumption level. It is increasing in the output share of tree i since the drop in aggregate consumption induced by a drop in tree i is larger if tree i represents a larger fraction of the economy. The second, smaller factor reflects the impact of jumps on the continuation utility via the state variables s_A and $\widehat{p}$. This factor becomes very large as $\widehat{p}$ moves towards 1. The impact of shocks on $\widehat{p}$, i.e. the probability update due to any kind of shock, is the highest if the agent is relatively certain to be in the calm state of the economy. The threat of contagion is thus priced most strongly if the investor is sure to be in the calm state. Taken together, the market price of jump risk is a decreasing function of s_i and $\widehat{p}$ as shown in the graph.

Given the market prices of risk and the price-dividend ratios of the dividend claims, i.e. the price exposures to the different risk factors, we can obtain their conditional expected excess returns. Here we analyze the results for asset A only, since the results for asset B are completely analogous.

Proposition 5. *The local expected excess return of asset A is determined by*

$$\Upsilon_A^{A,diff}\eta_A^{diff} + \Upsilon_A^{B,diff}\eta_B^{diff} - \widehat{\lambda}_A\Upsilon_A^{A,jump}\eta_A^{jump} - \widehat{\lambda}_B\Upsilon_A^{B,jump}\eta_B^{jump},$$

where the sensitivities with respect to the jump and Wiener processes, $\Upsilon_A^{A,diff}$, $\Upsilon_A^{B,diff}$, $\Upsilon_A^{A,jump}$ and $\Upsilon_A^{B,jump}$ are given in Appendix A.5.

The derivation is provided in Appendix A.5. The two middle graphs in Figure 3 depict the equity premium for the two dividend claims as a function of s_A and $\widehat{p}$. We also decompose the risk premium of asset A into the jump component and the diffusion component. We further decompose the diffusion risk premium into the cash flow component, the component due to s_A and the component due to $\widehat{p}$ in Figure 4.

We analyze the jump risk premium first. As documented by Branger, Kraft, and

Meinerding (2013a), the fact that consumption shocks and regime switches are coupled together via contagious shocks increases the jump risk premia disproportionately. However, this effect is weakened in an economy with only partial information. To get the intuition, consider first the hypothetical case where the agent has full information, i.e. she can observe the state of the economy perfectly. With partial information, every shock induces the same probability update, whereas with full information, there are either contagious jumps (which bring p to 0) or normal jumps (which do not affect p). In the full information case, the jump sizes of prices are thus effectively stochastic: a shock could either be contagious (with a larger price impact) or normal (with a smaller price impact). The jump risk premia in the full information case must therefore contain an additional risk premium related to the size of the jumps, which is not present with partial information. The total jump risk premium is therefore slightly lower in an economy with partial information, but still quite sizeable although we use rather moderate jump sizes in our calibration.

The diffusion risk premium can be decomposed into three terms, reflecting the three different components of the market prices of diffusive risk η_i^{diff}. The lower right graph of Figure 4 reveals that the uncertainty about the state of the economy adds a significant portion to the diffusion risk premium. For intermediate values of $\widehat{p}$, the premium for diffusive $\widehat{p}$ risk amounts to more than 6% and makes up the largest fraction of the total diffusion risk premium.

In summary, the analysis of the different types of risk premia shows that both of our key model assumptions have a strong impact on the equity premium. First, the existence of contagious shocks helps to generate a sizeable jump risk premium with rather frequent, but moderate jumps. This answers the concerns which have recently been raised by Constantinides (2008) or Backus, Chernov, and Martin (2011). Second, the additional layer of long-run risk introduced by the partial information feature of our model gives rise to a sizeable diffusion risk premium. Both components of the equity premium are concave in $\widehat{p}$, i.e. they are large in times of high uncertainty.

The Monte Carlo simulation gives a remarkable average excess return of 5.8 percentage points. Note that we include all realizations of negative shocks to the endowment (and hence to prices) in our sample and do not rely on a Peso problem story here. Moreover, note that the shocks in our model are very moderate, in line with evidence from Backus, Chernov, and Martin (2011) or Constantinides (2008). The reason for the still sizeable equity premium lies in our two key model features: contagious shocks increase jump risk premia disproportionately as has been explained by Branger, Kraft, and Mein-

erding (2013a). Learning and partial information on the other hand give rise to sizeable diffusion risk premia as well. Finally note that - although the price to fundamentals ratios are quite persistent - there is a fair amount of volatility even in the conditional expected excess return with a standard deviation of roughly 0.01. We will come back to this point when we analyze the predictability of returns.

4.5 Volatilities

Local second moments of the asset prices follow immediately from the price dynamics. Exact formulas are provided in Appendix A.5. The upper left graph of Figure 5 shows the local volatility of asset A as a function of s_A and $\widehat{p}$. The Figure also provides a decomposition into diffusion and jump parts.

As discussed above, uncertainty about the state of the economy induces additional diffusive volatility. This additional volatility is the highest for $\widehat{p} = 0.5$. Note that the output processes themselves have a diffusive volatility of 1%, which, with a leverage parameter of 2.5, increases to 2.5% for the dividends. The big boost then comes from adding uncertainty to the model, which produces a local diffusive price volatility of up to 13%.

Jump risk can contribute an equally large amount to the local volatility. On the one hand, the perceived jump intensity is decreasing in $\widehat{p}$, so that this fraction of the local volatility is rather high for $\widehat{p}$ close to zero. On the other hand, the impact of jumps on the estimated probability $\widehat{p}$ and thus on prices in the economy is the largest for intermediate values of $\widehat{p}$. Hence, the local volatility from jump risk is relatively high for intermediate values of $\widehat{p}$, but slightly declining as $\widehat{p}$ approaches 0. Again both central features of the model, contagious shocks and uncertainty about the economic state, are needed to generate a sizeable price volatility. Under the given calibration, the local volatility can exceed 18% if $\widehat{p}$ is around 0.5 and tree A makes up a large fraction of the economy, i.e. s_A is close to 1.

The simulation results in Table 2 document that the learning feature creates a significant amount of excess volatility in our model. The standard deviation of the return of the equity claim A in the simulations is about 0.124, whereas the dividend volatility is below 0.10. This excess volatility comes to a large extent from the volatility in the state variable $\widehat{p}$. Besides generating excess volatility per se, the learning mechanism in our model however also generates an interesting asymmetry in the excess volatility. This can best be seen from the exemplary sample paths in Figure 1. The noise in $\widehat{p}$ is way more pronounced for $\widehat{p}$ close to 0 than for $\widehat{p}$ close to 1. The reason is that it is almost

impossible for $\widehat{p}$ to approach the lower bound 0. Instead, during time periods where no jump is observed, there is always some drift upwards. If on the other hand $\widehat{p}$ approaches 1, there is no such drift in the other direction so that it is rather improbable for $\widehat{p}$ to take values significantly below 1.

This asymmetric – and in fact countercyclical – volatility of $\widehat{p}$ is transmitted to the return volatilities. To show this, we perform a regression exercise on our simulated data. We aggregate the returns of the risky asset A to obtain time series of monthly returns, then compute the volatilities of these monthly returns using a one, two, three or four-year rolling window and hence generate time series of volatilities of monthly returns.[12] Next, we integrate the simulated state variable $\widehat{p}$ over the same 1, 2, 3 or 4 years in order to generate time series of average estimated probabilities of being in the bad state. Intuitively, these time series measure the average perceived macroeconomic conditions over the estimation period. Finally, we regress the return volatilities on the integrated $\widehat{p}$.

The results from this exercise are reported in Table 3. To foster the intuition, we report annualized figures here. First, note that there is a substantial variation both in the integrated state variable $\widehat{p}$ and in the return volatilities which puts the integrated probability as an explanatory variable to a real test. Several studies in the literature have shown that return volatilities are strongly countercyclical.[13] Our model reproduces this stylized fact in the data. The slope coefficient in the regression for a time window of 1 year is -0.14 with a p-value below 0.01. If $\widehat{p}$ decreases from 1 to 0.5, i.e. contagion becomes quite likely to have occurred, the return volatilities go up by (annualized) 7 percentage points. The result of countercyclical volatilities is robust in various directions. Table 3 also reports the statistics if we extend the correlation window to 24, 36 or 48 months. The regression coefficient slightly increases in absolute value. We also performed the analysis with non-overlapping time periods, i.e., we computed one volatility for each year in the sample and then moved on to the next year. This leaves all the numbers practically unchanged.

4.6 Correlations

Next, we analyze the correlation between the returns of the two equity claims. Again, to grasp the whole picture, we have to analyze the conditional local correlations as well as the simulation results. As shown in the lower right graph of Figure 5, the presence

[12] The choice of monthly returns is motivated by the analysis in Mele (2007).

[13] See, e.g., Ehling and Heyerdahl-Larsen (2013) or Mele (2007) for results about US equity returns.

of state variables generates a nonzero local correlation. For all values of $\widehat{p}$, the fact that the output of both trees enters aggregate consumption (and thus the pricing kernel) induces correlation between their prices even though the fundamental cash flows are locally uncorrelated. This effect has also been documented by Cochrane, Longstaff, and Santa-Clara (2008) and Martin (2013). Moreover, the overall highest correlation (around 0.75) is again measured for intermediate values of $\widehat{p}$.

However, the graph also shows that the local correlation is smallest if the investor is sure to be in the bad state, i.e. if $\widehat{p}$ is close to 0. This seems counterfactual at first glance given, e.g., the evidence in Longin and Solnik (2001). The mechanism behind this result is as follows. With partial information every output shock, be it contagious or normal, has an effect on both the output share of tree A and on the state of the economy. On the other hand regime switches back from the contagion to the calm state are unobservable, these transitions do not affect the state variables s_A and $\widehat{p}$ locally. If $\widehat{p}$ is close to 0, the agent expects to see many non-contagious shocks (with relatively small impact on state variables) or a transition to the good state (with no direct impact on state variables at all). Since, on top of that, the diffusion correlation ρ is state-independent (and equal to zero), we observe the lowest local correlation for $\widehat{p} = 0$.

However, we would like to emphasize that in our opinion the local correlation is not the proper model-implied quantity to be compared to the data. Instead, we elaborate on the correlations of monthly returns in our simulated data. To do so, we repeat the regression exercise from the previous section. Instead of return volatilities, we now use correlations of monthly returns over 1, 2, 3 or 4 years as the dependent variable.[14] The results from this exercise are reported in Table 4. First of all, there is again a substantial variation both in the integrated state variable $\widehat{p}$ and in the correlation of monthly returns. The average correlation is between 0.47 and 0.60. Given that the two dividend processes are locally uncorrelated, this is already a stunning result. Longin and Solnik (2001) report an average correlation of 0.52 between monthly returns of US and UK stocks using data from January 1959 to December 1996. Ehling and Heyerdahl-Larsen (2013) analyze return correlations between several industries and report an average correlation of around 0.7. They also show that there is a substantial amount of heterogeneity and time variation in these correlations.

Both Longin and Solnik (2001) and Ehling and Heyerdahl-Larsen (2013) perform a battery of tests to show that return correlations are strongly countercyclical. This is

[14]The choice of monthly returns is motivated by the analysis in Longin and Solnik (2001).

exactly what our model produces. For a time window of 1 year, the slope coefficient in the regression is -0.38 with a p-value below 0.01. If $\widehat{p}$ decreases by 50%, i.e. contagion becomes more likely to have occurred, the monthly correlations go up by 19 percentage points. Although the local correlations in our model are procyclical, the realized correlations of monthly returns are highly countercyclical. Locally, all consumption shocks in our model are uncorrelated. But the jump intensities and also the drift rates depend on the economic state. Consequently, we see a lot of comovement in asset prices on the downside, but not so much on the upside, and this behavior cannot be captured by just looking at local correlations.

We accentuate that it is the interplay between all our key model ingredients that leads to this result. First of all, the contagion feature together with learning leads to patterns where both risky assets slide into a crisis together and stay there over a longer time period (see the exemplary sample paths in Figure 1). Second, the possibility of jumps and their increased frequency in the down state tilts the correlation towards countercyclicality. This would not be possible in a classical long-run risk setup or a Markov switching model where only the drift rates of consumption are time-varying. Note that the mechanism to generate countercyclical correlation in our model is also very different from the one in Martin (2013). In that paper, sudden 'correlation spikes' are generated by rare disasters like in Barro (2006) together with the usual spillover machinery in a two-tree framework, whereas we explicitly foreground the time dimension of crisis propagation.

The result of countercyclical correlations is again robust in various directions. Table 4 also reports the statistics if we extend the correlation window to 24, 36 or 48 months. The regression coefficient decreases in absolute value, but even for a horizon of 48 months it is still negative at -0.18 and significant. We also performed the analysis with non-overlapping time periods, i.e., we computed one correlation for each year in the sample and then moved on to the next year. This leaves all the numbers practically unchanged. Finally, we repeated the analysis with correlations of weekly returns instead of monthly returns. As this case is closer to the analysis of local correlations, the results become slightly weaker. We still observe regression coefficients of -0.35 and -0.17 for time windows of one and two years, respectively, but for longer time horizons the regression coefficients become insignificant.

4.7 Predictive Regressions

To investigate the properties of our model with respect to the predictability of future excess returns via the current value of the price-dividend ratio we first simulate the endowment processes and the state variable p with monthly increments for a total period length of 65 years. Then we compute the corresponding monthly price and return time series for the two risky assets A and B and for the claim to the aggregate dividends $D_{aggr} = D_A + D_B$ which we denote as the 'market portfolio'. Next, we aggregate the monthly returns to get annual time series. Finally, we run the following long horizon regressions:

$$\sum_{\tau=t}^{t+h-1} r_{aggr,\tau,\tau+1} - r_{f,\tau,\tau+1} = \alpha + \beta \; w_{aggr,t} + \varepsilon_t$$

where $r_{aggr,\tau,\tau+1}$ denotes the log return on the aggregate dividend claim from year τ to year $\tau + 1$, $r_{f,\tau,\tau+1}$ denotes the return on a risk-free bond from time τ to time $\tau + 1$ and $w_{aggr,t}$ is the log price-dividend ratio of the aggregate dividend claim at time t. Note that we proxy $r_{f,\tau,\tau+1}$ by integrating the monthly simulated risk-free short rates. We run the predictive regression for different horizons of $h = 1, 2, 4, 6, 8, 10$ years.

Table 5 reports the results. Panel A shows the results produced by our model for a sample length of 65 years.[15] Panel B gives the results reported in Wachter (2013) from a model with time-varying jump intensities. Panel C gives the numbers in the data which Wachter (2013) estimates for the period from 1947 to 2010.

The betas in our model are extremely close to those reported in Wachter (2013) and also close to the data, between -0.19 and -0.64. This is not surprising given the fact that most models with recursive utility and long-run risk variables are able to generate return predictability. Future average returns in our model depend on the current values of s_A and $\widehat{p}$, i.e. on the expectation of future jumps, and so do current price-dividend ratios. This creates betas which increase with the regression horizon. The R^2 values do not match the empirical values. But as Wachter (2013) already points out, the R^2 would be considerably higher if we could exclude the realized jumps from our sample. Upon a jump in the dividend, most of the excess return variation comes from the change in dividends and not from a movement in the price-dividend ratio. Unfortunately, we cannot do that type of analysis here because jumps are much more frequent in our model than in Wachter (2013).

We repeat the predictive regressions with consumption growth rates as the left-

[15] We repeat the procedure described above 1,000 times and report the mean of the estimated betas.

hand variable, the results are reported in Table 6. The numbers are again closely in line with the data in the sense that the price-dividend ratio does not predict consumption growth. This finding is in stark contrast to typical long-run risk models like Bansal and Yaron (2004), and our model performs even better than the model of Wachter (2013).[16] Not only are the betas close to zero and independent of the time horizon of the regression. On top of that, the R^2's are considerably low and much closer to the data than in other long-run risk models.

The fact that consumption growth rates are unpredictable both for long and short horizons has two reasons. First of all, the timing of the shocks cannot be predicted by the price-dividend ratio at all. But short-horizon consumption growth rates are heavily affected by the realization of jumps and there are relatively many of them in our sample because of the rather high jump intensities. This eliminates nearly all predictability for short maturities. For long-horizon consumption growth, a second effect comes into play. Our state variable $\widehat{p}$ is not a long-run risk variable in the original sense. Table 2 reports an annual autocorrelation of 0.46 for $\widehat{p}$ which is way below the autocorrelation of long-run risk variables like the ones in Bansal and Yaron (2004) or Wachter (2013). Note, e.g., that the average length of a contagion period is 1 year in our benchmark calibration and that $\widehat{p}$ reverts back to 0 rather quickly once a contagion period has ended (see the paths in Figure 1). The lack of persistence in the state variable $\widehat{p}$ implies that long-horizon consumption growth rates depend much less on the economic state which prevailed at the beginning of the period. As a result, long-horizon consumption growth rates are unpredictable, too. Both the betas and the R^2 stay low for very long horizons.

To sum up, our model is thus able to shut down the counterfactually high consumption growth predictability which is introduced by long-run risk in many recent papers. Nevertheless, we are still able to generate enough return predictability. Finally, we wish to stress that we do not have to sacrifice much of the autocorrelation of price-to-fundamentals ratios to achieve this result. E.g., Table 2 reports annual autocorrelations of the price-dividend ratios of the single trees of 0.74. As will become clear below, we can further increase the persistence of the price-dividend ratios, especially for small trees, if we make use of our two-tree setup and allow for heterogeneous trees.

[16] We redid the analysis with dividend growth instead of consumption growth, and price-dividend ratios also do not predict dividend growth in our model. The results are not shown to save space.

4.8 Term Structure of Equity

There is a growing body of literature about the term structure of returns and volatilities of equity claims. Most prominently, van Binsbergen, Brandt, and Koijen (2012) argue that the term structure of equity returns and volatilities is downward-sloping. Boguth, Carlson, Fisher, and Simutin (2012), on the other hand, argue that tiny market frictions might be the reason for this behavior. Nevertheless, there is a rising number of papers trying to explain the negative slope, e.g. Lettau and Wachter (2007).

Following Belo, Collin-Dufresne, and Goldstein (2012), we define a dividend strip to be a claim on the value of the dividend at time T. Its value at time t is given by

$$V_A^T(t) = E_t^{\mathbf{Q}}\left[e^{-\int_t^T r_{f,s}ds} D_{A,T}\right] = E_t\left[\frac{\xi_T}{\xi_t} D_{A,T}\right].$$

Using standard arguments (see Appendix A.6) we can derive a partial differential equation for the log price-dividend ratio $y_{A,t} = \log \frac{V_A^T(t)}{D_t}$ of this dividend strip. This partial differential equation has properties similar to the differential equations discussed before, except that there is now also a time derivative because the maturity of the dividend strip is finite. We solve it numerically, iterating backwards in time starting from the boundary condition $y_A^T(T) = 0$. Given the numerical solution of the price-dividend ratio, we derive the dynamics of $V_A^T(t)$ using Itô's Lemma and compute conditional moments similar to what we did for the equity claims in Section 3. In the following, we will focus on the local expected excess return and local volatility as functions of the time to maturity $T - t$.

Figure 6 depicts the term structures for maturities up to 40 years and for different values of $\widehat{p}$ between 0 and 1. Results not reported here indicate that there is more variation due to changes in $\widehat{p}$ than due to s_A, we therefore stick to $s_A = 0.5$ in the following analysis. The term structure of volatilities exhibits a slightly hump-shaped pattern for $\widehat{p} \geq 0.2$. However, the hump decreases in $\widehat{p}$ and for $\widehat{p} = 0$ the term structure of volatilities is completely decreasing. The expected excess returns are increasing with maturity for all $\widehat{p} \geq 0.2$, but they seem to stabilize from about 3 years onwards, which is consistent with the hump in the volatilities around the same maturity. Finally, the term structure of equity risk premia is completely flat for $\widehat{p} = 0$.

The mechanism at work here is similar to the one in Croce, Lettau, and Ludvigson (2012). The term structure of equity returns is typically upward-sloping in long-run risk models because of the eponymous long-term character of the risk factors involved.[17] Croce,

[17] See the evidence in van Binsbergen, Brandt, and Koijen (2012) or Wachter (2013).

Lettau, and Ludvigson (2012) however point out that partial information about long-run risk has the potential to reduce the upward slope or even induce a downward slope. The reason is that a partially informed agent filters the current value of the long-run risk variable from observables. These observables (typically consumption or dividends) depend on both short-run and long-run risk, and so the agent always underestimates the degree of long-run risk and overestimates the degree of short-run risk in the economy. As a result, the term structure of equity is twisted and can even become downward-sloping. In our model, the diffusive and jump risk in the endowment processes can be seen as short-run risk. Long-run risk is represented by the two state variables s_A and $\widehat{p}$. Since these two variables are only slightly persistent (compare the discussion above), our model does not show up a large amount of long-run risk to begin with. But in principle, contagious jumps induce additional long-run risk in the economy. The fact that the agent cannot identify these contagious jumps perfectly however reduces the effect of these jumps exactly as in Croce, Lettau, and Ludvigson (2012). Therefore, in contrast to the model of Wachter (2013), in which the time-varying disaster risk serves as the long-run risk variable, the term structure of equity yields is approximately flat from 3 years onwards. This intuition is confirmed by robustness checks where we compute the term structure of equity for higher diffusion volatilities σ_A and σ_B. Higher volatilities imply that the signals C_A and C_B are less informative and hence the probability $\widehat{p}$ is estimated with smaller precision. The effect of learning on the slope of the term structure should be larger in more volatile economies. Our results indeed show that the term structure of equity becomes flatter with increasing σ_A and σ_B.[18]

4.9 Autocorrelations and Cross-Sectional Analysis

The above analysis has shown that the success of our model concerning predictive regressions is due to the fact that the price-dividend ratios are rather persistent, although the state variables themselves are not. This autocorrelation is especially pronounced for the claims to the individual dividend streams D_A and D_B as compared to the claim on

[18] Another way to figure out the intuition behind the term structure of equity is given by the approach of Lettau and Wachter (2007) who try to explain the term structure of equity and interest rates via 'reverse engineering'. Their results show that the slope of the term structure of equity can be negative if the correlations between the market prices of risk and the expected dividend growth rates are negative. From Figure 3, one can deduce that the correlation between expected dividend growth and the market price of jump risk is mostly positive. The correlation between expected dividend growth and the market price of diffusion risk is ambiguous. Altogether, the slope of the term structure of equity is thus positive and approaching zero for long horizons.

aggregate dividends $D_A + D_B$. We will now elaborate a bit more on this aspect by allowing for heterogeneity among the two trees.

Our model enables us to study the equilibrium effects of heterogeneity within one single economy whereas, in a one-tree economy, we could only compare different market equilibria, depending on the parametrization of that single tree. As will become clear below, this has first-order consequences for the autocorrelations, but also for expected returns, return volatilities and correlations.

We do the analysis in two steps. First, we keep the parametrization fixed and stick to the benchmark calibration, but we change the relative sizes of the trees. Until now, we started our Monte Carlo simulation with equally large trees, i.e. $s_{A,0} = 0.5$. Since consumption does not move very much, it is very unlikely to reach more extreme values of s_A within the 65 years simulation window. Therefore, we redo the Monte Carlo simulation with starting values $s_{A,0}$ equal to 0.67, 0.75, and 0.83, respectively. In the second step, we allow for parameters different from the benchmark case, but start the simulation with s_A equal to 0.5 again. The parameters for these three additional cases are shown in Table 1.

4.9.1 Different Tree Sizes

The results from the first exercise are reported in the last three columns of Table 2 where we vary the starting values for s_A. Apparently, as the economy becomes more imbalanced, the price-dividend ratio of the smaller tree B becomes more persistent with first-order autocorrelation up to 0.82. At the same time, the price-dividend ratio of the larger tree A becomes less persistent. Nevertheless, the autocorrelation of the market price-dividend ratio increases to 0.79. The autocorrelation of the wealth-consumption ratio goes up as well, it reaches 0.57 for the most extreme case. The more imbalanced economies are thus closer to the data in this respect. The numbers generated by our model are close to what is usually observed in long-run risk models as shown by Bansal, Kiku, Shaliastovich, and Yaron (2013).

This autocorrelation pattern has its root in the correlation between the state variables s_A and $\widehat{p}$. To see this, assume for simplicity that the price-dividend ratio of asset B can locally be approximated by some affine function of the state variables:

$$e^{\omega_{B,t}} \approx a_t s_{A,t} + b_t \widehat{p}_t \tag{9}$$

Then the time series autocorrelation $corr\left(e^{\omega_{B,t}}, e^{\omega_{B,t+1}}\right)$ not only depends on the individ-

ual autocorrelations of s_A and $\widehat{p}$, but also on the interaction terms $corr(s_{A,t}, \widehat{p}_{t+1})$ and $corr(\widehat{p}_t, s_{A,t+1})$. Now suppose that asset B is small, i.e. s_A is close to 1. In this case, the correlations $corr(s_{A,t}, \widehat{p}_{t+1})$ and $corr(\widehat{p}_t, s_{A,t+1})$ are positive. To see this note that shocks in C_A and C_B have asymmetric effects on s_A when asset B is small, while the effect on $\widehat{p}$ is always symmetric. A large negative shock in $C_{A,t}$ reduces both $s_{A,t}$ and $\widehat{p}_t$ drastically, but a large negative shock in $C_{B,t}$ increases $s_{A,t}$ only slightly. Since s_A and $\widehat{p}$ themselves have mildly positive autocorrelations, this results in positive correlations $corr(s_{A,t}, \widehat{p}_{t+1})$ and $corr(\widehat{p}_t, s_{A,t+1})$. Moreover, Figure 2 show that the loading a_t is large and positive if s_A is close to 1. Together with the positive interaction terms $corr(s_{A,t}, \widehat{p}_{t+1})$ and $corr(\widehat{p}_t, s_{A,t+1})$, this gives rise to additional autocorrelation $corr\left(e^{\omega_{B,t}}, e^{\omega_{B,t+1}}\right)$ as compared to a model where the two state variables were independent. The somewhat lower autocorrelation of the large asset A can be explained with a similar argument.

To sum up, in a framework with two Lucas trees and an additional state variable like $\widehat{p}$, the price-dividend ratios of small trees are more persistent than those of large trees, which we can also see from the numbers in Table 2. In addition it is not only the autocorrelation for the small tree which increases (up to 0.82 for very large starting value of s_A), but we also see additional persistence in the price-dividend ratio of the 'market portfolio', i.e. the claim to aggregate dividends $D_A + D_B$. Thus, the autocorrelation of the market portfolio is not just a weighted average of the two individual autocorrelations, but it is tilted towards the autocorrelation of the small tree as the economy becomes more and more imbalanced.

4.9.2 Heterogeneity with Respect to Cash Flow Dynamics

We finally analyze the implications of heterogeneity between the trees with respect to their cash flow dynamics. More precisely we look at three additional cases the parameters for which are reported in the last three columns of Table 1. The asset pricing moments are summarized in Table 7.

In the first scenario, we change the jump intensities of the trees in the calm state. The total jump intensity of each tree remains the same. However, tree A now exhibits only contagious shocks while tree B only suffers from normal jumps. The local distribution of consumption does not change compared to the benchmark case. However, asset A is now very 'toxic' in the sense that it is very likely to trigger a crisis, while asset B is not. Note that in this setup learning becomes less important as contagious jumps can be identified perfectly.

The second calibration focusses on differences in the jump intensities in the contagion state. Tree A represents a more robust sector of the economy which exhibits a lower jump intensity in the contagion state, while tree B is very contagion-sensitive with a jump intensity of 0.95. Again, the local distribution of aggregate consumption does not change compared to the benchmark case.

Finally, we analyze the impact of the drift rates of the trees. The agent in our model filters the latent state of the economy from the observation of diffusion and jumps. In this third variation of the base case we choose the drift rates such that tree A has a larger drift spread between calm and contagion state than tree B. Observations of realizations of tree A will thus be more informative about the economic state than those of tree B and hence tree A will have a higher impact on the state variable $\widehat{p}$. The different influence on $\widehat{p}$ will thus affect the fraction of systemic risk carried by both assets.

The results in Table 7 show that parameter heterogeneity affects in particular three moments: the autocorrelation of price-dividend ratios and thus of expected returns, the expected returns themselves and the return volatilities. The autocorrelation patterns follow from the connection between state variables and price-dividend ratios again. Suppose asset A is robust and asset B is contagion-sensitive. The loading b_t in equation (9) is then much larger for the contagion-sensitive asset B. Moreover, the output share s_A tends to increase slightly over time. The combination of these two effects explains the extreme autocorrelation of 0.97 in the sample. This finding shows again that it is crucial to have two Lucas trees in the model. Heterogeneity of the trees with respect to the crisis propagation mechanism can add another significant portion of autocorrelation and bring the model even closer to the data.

Parameter heterogeneity also affects expected returns. Consider first the case of a toxic asset A and a non-toxic asset B where all jumps in tree A are contagious, while all jumps in tree B are normal. Since the compensation for the risk of contagious jumps is significantly greater than that for normal jumps, asset A commands a higher jump risk premium in this case. For the other two cases, we also see an additional risk premium for asset A. Here, s_A also tends to increase slightly over time. As described in the previous section, risk premia are generally larger for those assets which have a high output share. In summary, we see the highest risk premium for an asset which has a large spread in the drift rate μ due to contagion. Its premium can be twice as high as the one for the small growth spread asset.

5 Conclusion

In this paper we analyze the general equilibrium pricing effects of uncertainty about the propagation of shocks in a two-sector economy. This uncertainty relates to the state of the economy, which can be either calm or contagious, but is unobservable for the investor who has to filter it from the data. The propagation of shocks itself is modeled by endowment jumps which simultaneously trigger a regime shift to a bad economic state. It is important to note that we do not assume some sort of common simultaneous jumps across the two trees, but we interpret a crisis as something with a distinct time dimension to it, i.e., not a single event, but a sequence of negative shocks with potentially long-lasting effects on the economy as a whole.

In our model the two channels of shock propagation and unobservability of the state generate a number of interesting asset pricing implications, and the endogenously generated properties of prices, returns, and volatilities fit the data along several dimensions quite well. Via the shock propagation channel we generally obtain higher risk premia and a lower risk-free rate. Incomplete information about the state of the economy helps to explain second moments of asset prices. The additional uncertainty increases the diffusion part of return volatilities substantially and helps explaining the excess volatility of equity returns. Moreover, the return volatilities are highly countercyclical as in the data. Concerning return predictability the model is close to the data in the sense that future excess returns are predictable, whereas consumption or dividend growth is not predictable at all.

Having two trees in the economy allows us to study equilibrium return correlations. We assume locally uncorrelated fundamentals, so that all the correlation between the two sectors is generated endogenously by the equilibrium pricing mechanism. The correlation between the two sectors in our economy is strongly countercyclical, i.e., it increases dramatically in the bad, contagious state of the economy relative to the good, calm state. This is a stylized fact often observed in empirical studies, and our model provides a rationale for why correlations actually might go up in bad times.

We also study the effects of heterogeneity between the two sectors of the economy on asset prices. In the base case these sectors are assumed to be identical, but we find that introducing asymmetry in either the parametrization or in the size of the sectors is essential for bringing the autocorrelations of the price-to-fundamentals ratios closer to the data. Note that the state variables in our model have relatively low persistence which helps us to get rid of the counterfactual consumption growth predictability. It is exactly

the interplay of our crisis propagation mechanism with the two-tree framework which helps us bringing the autocorrelations to reasonable levels.

Finally, there is growing interest in the literature in the properties of expected excess returns and volatilities of claims to a single dividend paid at different times in the future, the so-called term structure of equity. Our model generates risk premia for these dividend strips which increase with maturity, but at a decreasing rate, and essentially become flat from a horizon of 3 years on. The term structure of return volatilities on these assets is in most scenarios hump-shaped, i.e., tends to decrease with increasing maturity beyond a certain horizon. It is predominantly the unobservability of the economic state driving these results, which are well in line with the data.

Overall, our model provides a realistic mechanism through which a crisis can spread across several sectors of the economy. Topics for future research could be to place the model in an international context which would introduce exchange rate risk and would allow to study the differential pricing of equity claims in countries, which are more or less likely to cause contagious shocks.

A Proofs

A.1 Filter Equation

The following proof follows along the lines of Branger, Kraft, and Meinerding (2013b). The consumption dynamics under the full filtration $\mathcal{F}$ are given by

$$\begin{pmatrix} \frac{dC_{A,t}}{C_{A,t-}} \\ \frac{dC_{B,t}}{C_{B,t-}} \end{pmatrix} = \begin{pmatrix} \mu_{A,t} \\ \mu_{B,t} \end{pmatrix} dt + \Sigma_{AB} \begin{pmatrix} dW_{A,t} \\ dW_{B,t} \end{pmatrix} + \begin{pmatrix} L_A \left(dN_{A,t}^{calm,calm} + dN_{A,t}^{calm,cont} + dN_{A,t}^{cont,cont} \right) \\ L_B \left(dN_{B,t}^{calm,calm} + dN_{B,t}^{calm,cont} + dN_{B,t}^{cont,cont} \right) \end{pmatrix},$$

where $\Sigma_{AB} = \begin{pmatrix} \sigma_A & 0 \\ 0 & \sigma_B \end{pmatrix}$ and the Wiener Processes $W_{A,t}$ and $W_{B,t}$ are correlated with correlation ρ. In order to be able to apply the theorems from Frey and Runggaldier (2010), we rewrite the dynamics slightly using independent Wiener processes W_1 and W_2:

$$\begin{pmatrix} \frac{dC_{A,t}}{C_{A,t-}} \\ \frac{dC_{B,t}}{C_{B,t-}} \end{pmatrix} = \begin{pmatrix} \mu_{A,t} \\ \mu_{B,t} \end{pmatrix} dt + \Sigma \begin{pmatrix} dW_{1,t} \\ dW_{2,t} \end{pmatrix} + \begin{pmatrix} L_A \left(dN_{A,t}^{calm,calm} + dN_{A,t}^{calm,cont} + dN_{A,t}^{cont,cont} \right) \\ L_B \left(dN_{B,t}^{calm,calm} + dN_{B,t}^{calm,cont} + dN_{B,t}^{cont,cont} \right) \end{pmatrix}$$

with $\Sigma = \begin{pmatrix} \sigma_A & 0 \\ \rho\sigma_B & \sqrt{1-\rho^2}\sigma_B \end{pmatrix}$ and $\Sigma\Sigma^T = \begin{pmatrix} \sigma_A^2 & \rho\sigma_A\sigma_B \\ \rho\sigma_A\sigma_B & \sigma_B^2 \end{pmatrix}$. The relation between the Wiener processes is given by

$$\begin{pmatrix} dW_{1,t} \\ dW_{2,t} \end{pmatrix} = \Sigma^{-1}\Sigma_{AB} \begin{pmatrix} dW_{A,t} \\ dW_{B,t} \end{pmatrix}.$$

The same equation holds for the perceived Wiener processes $\widehat{W}$. Under the investor's filtration $\mathcal{G}$, the consumption dynamics are

$$\begin{pmatrix} \frac{dC_{A,t}}{C_{A,t-}} \\ \frac{dC_{B,t}}{C_{B,t-}} \end{pmatrix} = \begin{pmatrix} \widehat{\mu}_{A,t} \\ \widehat{\mu}_{B,t} \end{pmatrix} dt + \Sigma \begin{pmatrix} d\widehat{W}_{1,t} \\ d\widehat{W}_{2,t} \end{pmatrix} + \begin{pmatrix} L_A d\widehat{N}_{A,t} \\ L_B d\widehat{N}_{B,t} \end{pmatrix}.$$

The subjective drift and jump intensity of asset $i = A, B$ are given by

$$\begin{aligned} \widehat{\mu}_i &= \widehat{p}_t \mu_i^{calm} + (1-\widehat{p}_t)\mu_i^{cont} \\ \widehat{\lambda}_i &= \widehat{p}_t \left(\lambda_i^{calm,calm} + \lambda_i^{calm,cont} \right) + (1-\widehat{p}_t)\lambda_i^{cont,cont}, \end{aligned}$$

where $\widehat{p}_t$ denotes the subjective probability of being in the calm state at time t. Note that the diffusion volatilities and correlations do not depend on the state of the economy and are known to the investor. The Brownian motions $\widehat{W}_i$ are related to W_i via

$$d\widehat{W}_t = dW_t + \Sigma^{-1} \begin{pmatrix} \mu_{A,t} - \widehat{\mu}_{A,t} \\ \mu_{B,t} - \widehat{\mu}_{B,t} \end{pmatrix} dt,$$

and the observable jumps are given by

$$\widehat{N}_{i,t} = N_{i,t}^{calm,calm} + N_{i,t}^{calm,cont} + N_{i,t}^{cont,cont}, \quad i \in \{A, B\}.$$

To deduce the filter equation we build on the results of Frey and Runggaldier (2010). Our model can be viewed as a special case of theirs. The subjective probability of being in the calm state, $\widehat{p}$, can be written as

$$\widehat{p} = \frac{\sigma^{calm}}{\sigma^{cont} + \sigma^{calm}}.$$

The processes σ^{calm} and σ^{cont} then satisfy so-called Zakai equations. Applying Proposition 4.1, Corollary 4.2 and Algorithm 4.3 from Section 4 of Frey and Runggaldier (2010), we obtain the Zakai equations

$$\begin{aligned}
d\sigma_t^{calm} = &- \sum_{i=A,B} \left(\lambda_i^{calm,calm} + \lambda_i^{calm,cont}\right) \sigma_t^{calm} dt + \lambda^{cont,calm} \sigma_t^{cont} dt \\
&+ \sigma_t^{calm} \begin{pmatrix} \mu_A^{calm} & , & \mu_B^{calm} \end{pmatrix} (\Sigma\Sigma^T)^{-1} \left[\frac{\sigma_t^{calm}}{\sigma_t^{cont} + \sigma_t^{calm}} \begin{pmatrix} \mu_A^{calm} \\ \mu_B^{calm} \end{pmatrix} + \frac{\sigma_t^{cont}}{\sigma_t^{cont} + \sigma_t^{calm}} \begin{pmatrix} \mu_A^{cont} \\ \mu_B^{cont} \end{pmatrix} \right] dt \\
&+ \sigma_t^{calm} \begin{pmatrix} \mu_A^{calm} & , & \mu_B^{calm} \end{pmatrix} (\Sigma\Sigma^T)^{-1} \Sigma d\widehat{W}_t \\
&+ \sum_{i=A,B} \left(\frac{\lambda_i^{calm,calm} \sigma_{t-}^{calm}}{\lambda_i^{cont,cont} \sigma_{t-}^{cont} + (\lambda_i^{calm,calm} + \lambda_i^{calm,cont}) \sigma_{t-}^{calm}} - \sigma_{t-}^{calm} \right) d\widehat{N}_{i,t},
\end{aligned}$$

and

$$\begin{aligned}
d\sigma_t^{cont} = &- \sum_{i=A,B} \lambda_i^{cont,cont} \sigma_t^{cont} dt - \lambda^{cont,calm} \sigma_t^{cont} dt \\
&+ \sigma_t^{cont} \begin{pmatrix} \mu_A^{cont} & , & \mu_B^{cont} \end{pmatrix} (\Sigma\Sigma^T)^{-1} \left[\frac{\sigma_t^{calm}}{\sigma_t^{cont} + \sigma_t^{calm}} \begin{pmatrix} \mu_A^{calm} \\ \mu_B^{calm} \end{pmatrix} + \frac{\sigma_t^{cont}}{\sigma_t^{cont} + \sigma_t^{calm}} \begin{pmatrix} \mu_A^{cont} \\ \mu_B^{cont} \end{pmatrix} \right] dt \\
&+ \sigma_t^{cont} \begin{pmatrix} \mu_A^{cont} & , & \mu_B^{cont} \end{pmatrix} (\Sigma\Sigma^T)^{-1} \Sigma d\widehat{W}_t \\
&+ \sum_{i=A,B} \left(\frac{\lambda_i^{cont,cont} \sigma_{t-}^{cont} + \lambda_i^{calm,cont} \sigma_{t-}^{calm}}{\lambda_i^{cont,cont} \sigma_{t-}^{cont} + (\lambda_i^{calm,calm} + \lambda_i^{calm,cont}) \sigma_{t-}^{calm}} - \sigma_{t-}^{cont} \right) d\widehat{N}_{i,t}.
\end{aligned}$$

We then apply Itô's Lemma to $\widehat{p} = \frac{\sigma^{calm}}{\sigma^{cont} + \sigma^{calm}}$. After some manipulations, we arrive at

$$\begin{aligned}
d\widehat{p}_t = &\left((1 - \widehat{p}_t) \lambda^{cont,calm} - \widehat{p}_t (\lambda_A^{calm,cont} + \lambda_B^{calm,cont}) \right) dt \\
&+ \widehat{p}_t (1 - \widehat{p}_t) \begin{pmatrix} \mu_A^{calm} - \mu_A^{cont} & , & \mu_B^{calm} - \mu_B^{cont} \end{pmatrix} \left(\Sigma^{-1}\right)^T d\widehat{W}_t \\
&+ \left(\frac{\widehat{p}_{t-} \lambda_A^{calm,calm}}{\widehat{\lambda}_{A,t}} - \widehat{p}_{t-} \right) \left(d\widehat{N}_{A,t} - \widehat{\lambda}_{A,t} dt \right) + \left(\frac{\widehat{p}_{t-} \lambda_B^{calm,calm}}{\widehat{\lambda}_{B,t}} - \widehat{p}_{t-} \right) \left(d\widehat{N}_{B,t} - \widehat{\lambda}_{B,t} dt \right).
\end{aligned}$$

As we have formulated the dynamics of the consumption trees with respect to the correlated Wiener processes $\widehat{W}_A$ and $\widehat{W}_B$ we will finally rewrite the dynamics for $\widehat{p}$ also in terms of these correlated Wiener

processes:

$$
\begin{aligned}
d\widehat{p}_t = &\left((1-\widehat{p}_t)\lambda^{cont,calm} - \widehat{p}_t(\lambda_A^{calm,cont} + \lambda_B^{calm,cont})\right) dt \\
&+ \widehat{p}_t(1-\widehat{p}_t)\left(\begin{array}{ccc} \mu_A^{calm} - \mu_A^{cont} & , & \mu_B^{calm} - \mu_B^{cont} \end{array}\right)\left(\Sigma\Sigma^T\right)^{-1}\Sigma_{AB}\left(\begin{array}{c} d\widehat{W}_{A,t} \\ d\widehat{W}_{B,t} \end{array}\right) \\
&+ \left(\frac{\widehat{p}_{t-}\lambda_A^{calm,calm}}{\widehat{\lambda}_{A,t}} - \widehat{p}_{t-}\right)\left(d\widehat{N}_{A,t} - \widehat{\lambda}_{A,t}dt\right) + \left(\frac{\widehat{p}_{t-}\lambda_B^{calm,calm}}{\widehat{\lambda}_{B,t}} - \widehat{p}_{t-}\right)\left(d\widehat{N}_{B,t} - \widehat{\lambda}_{B,t}dt\right).
\end{aligned}
$$

Note that

$$
\left(\Sigma\Sigma^T\right)^{-1}\Sigma_{AB} = \left(\begin{array}{cc} \frac{1}{(1-\rho^2)\sigma_A} & -\frac{\rho}{(1-\rho^2)\sigma_A} \\ -\frac{\rho}{(1-\rho^2)\sigma_B} & \frac{1}{(1-\rho^2)\sigma_B} \end{array}\right).
$$

A.2 Wealth-Consumption Ratio

The representative agent's value function depends on the filtered probability $\widehat{p}$ and the output share s_A and is given by

$$
J_t = E_t\left[\int_t^\infty f(C_s, J_s)ds\right].
$$

As in Duffie and Epstein (1992b), the aggregator f is defined as

$$
f(C,J) = \frac{\beta C^{1-\frac{1}{\psi}}}{\left(1-\frac{1}{\psi}\right)\left[(1-\gamma)J\right]^{\frac{1}{\theta}-1}} - \beta\theta J.
$$

Following Duffie and Epstein (1992a), the Bellman equation for stochastic differential utility reads

$$
0 = f(C_t, J_t) + \mathcal{D}J_t. \tag{A.1}
$$

We apply the following functional form for the value function J:

$$
J = \frac{C^{1-\gamma}}{1-\gamma}\beta^\theta e^{\theta v}, \tag{A.2}
$$

where v is a twice differentiable function in both the output share s_A and the filtered probability $\widehat{p}$.[19] Plugging the guess $(A.2)$ into the aggregator function gives

$$
f(C,J) = \theta J\left(e^{-v} - \beta\right). \tag{A.3}
$$

[19] Campbell, Chacko, Rodriguez, and Viceira (2004) show that v is then equal to the logarithm of the wealth-consumption ratio.

The infinitesimal generator $\mathcal{D}J$ under the investor's filtration $\mathcal{G}$ follows from an application of Itô's Lemma:

$$\begin{aligned}\mathcal{D}J = &\frac{\partial J}{\partial C}dC + \frac{1}{2}\frac{\partial^2 J}{\partial C^2}d\langle C\rangle + \frac{\partial J}{\partial s_A}ds_A + \frac{1}{2}\frac{\partial^2 J}{\partial s_A^2}d\langle s_A\rangle + \frac{\partial J}{\partial \widehat{p}}d\widehat{p} + \frac{1}{2}\frac{\partial^2 J}{\partial \widehat{p}^2}d\langle \widehat{p}\rangle \\ &+ \frac{\partial^2 J}{\partial C \partial s_A}d\langle C, s_A\rangle + \frac{\partial^2 J}{\partial C \partial \widehat{p}}d\langle C, \widehat{p}\rangle + \frac{\partial^2 J}{\partial \widehat{p}\partial s_A}d\langle \widehat{p}, s_A\rangle \\ &+ \sum_{i=A,B}\widehat{\lambda}_i\left(\frac{(C^{i+})^{1-\gamma}}{1-\gamma}\beta^\theta e^{\theta v(s_A^{i+},\widehat{p}^{i+})} - \frac{C^{1-\gamma}}{1-\gamma}\beta^\theta e^{\theta v(s_A,\widehat{p})}\right).\end{aligned}$$

Computing the derivatives of J with respect to C, s_A and $\widehat{p}$ gives

$$\begin{aligned}\mathcal{D}J = &\left(1-\frac{1}{\psi}\right)\theta J\mu_C - \frac{1}{2}\gamma\left(1-\frac{1}{\psi}\right)\theta J\sigma_{CC} \\ &+ v_s\theta J\mu_s + \frac{1}{2}\theta J\left(v_{ss} + \theta(v_s)^2\right)\sigma_{ss} + v_{\widehat{p}}\theta J\mu_{\widehat{p}} + \frac{1}{2}\theta J\left(v_{\widehat{p}\widehat{p}} + \theta(v_{\widehat{p}})^2\right)\sigma_{\widehat{p}\widehat{p}} \\ &+ (1-\gamma)\theta J v_s\sigma_{Cs} + (1-\gamma)\theta J v_{\widehat{p}}\sigma_{C\widehat{p}} + \theta J\left(v_{s\widehat{p}} + \theta v_s v_{\widehat{p}}\right)\sigma_{s\widehat{p}} \\ &+ \sum_{i=A,B}\widehat{\lambda}_i J\left[(1+s_iL_i)^{1-\gamma}e^{\theta v(s_A^{i+},\widehat{p}^{i+})-\theta v(s_A,\widehat{p})} - 1\right],\end{aligned}$$

where we use the shortcuts

$$\mu_C = s_A\widehat{\mu}_A + s_B\widehat{\mu}_B \tag{A.4}$$

$$\sigma_{CC} = s_A^2\sigma_A^2 + s_B^2\sigma_B^2 + 2\rho s_A s_B\sigma_A\sigma_B \tag{A.5}$$

$$\mu_s = s_A s_B\left[\widehat{\mu}_A - \widehat{\mu}_B - s_A\sigma_A^2 + s_B\sigma_B^2 + (s_A - s_B)\rho\sigma_A\sigma_B\right] \tag{A.6}$$

$$\sigma_{ss} = s_A^2 s_B^2\left[\sigma_A^2 + \sigma_B^2 - 2\rho\sigma_A\sigma_B\right] \tag{A.7}$$

$$\mu_{\widehat{p}} = (1-\widehat{p})\lambda^{cont,calm} - \widehat{p}\left(\lambda_A^{calm,cont} + \lambda_B^{calm,cont}\right) - \widehat{\lambda}_A\left(\frac{\widehat{p}\lambda_A^{calm,calm}}{\widehat{\lambda}_A} - \widehat{p}\right) - \widehat{\lambda}_B\left(\frac{\widehat{p}\lambda_B^{calm,calm}}{\widehat{\lambda}_B} - \widehat{p}\right) \tag{A.8}$$

$$\sigma_{\widehat{p}\widehat{p}} = \widehat{p}^2(1-\widehat{p})^2\left[\frac{(\mu_A^{calm} - \mu_A^{cont})^2}{(1-\rho^2)\sigma_A^2} - \frac{2\rho(\mu_A^{calm} - \mu_A^{cont})(\mu_B^{calm} - \mu_B^{cont})}{(1-\rho^2)\sigma_A\sigma_B} + \frac{(\mu_B^{calm} - \mu_B^{cont})^2}{(1-\rho^2)\sigma_B^2}\right] \tag{A.9}$$

$$\sigma_{Cs} = s_A s_B\left[s_A\sigma_A^2 - s_B\sigma_B^2 - \rho s_A\sigma_A\sigma_B + \rho s_B\sigma_A\sigma_B\right] \tag{A.10}$$

$$\sigma_{C\widehat{p}} = \widehat{p}(1-\widehat{p})\left[s_A(\mu_A^{calm} - \mu_A^{cont}) + s_B(\mu_B^{calm} - \mu_B^{cont})\right] \tag{A.11}$$

$$\sigma_{s\widehat{p}} = \widehat{p}(1-\widehat{p})s_A s_B\left[(\mu_A^{calm} - \mu_A^{cont}) - (\mu_B^{calm} - \mu_B^{cont})\right]. \tag{A.12}$$

Plugging DJ into the Bellman equation $(A.1)$ gives a PDE for the log wealth-consumption ratio v:

$$\begin{aligned}0 = &e^{-v} - \beta + \left(1-\frac{1}{\psi}\right)\mu_C - \frac{1}{2}\gamma\left(1-\frac{1}{\psi}\right)\sigma_{CC} \\ &+ v_s\mu_s + \frac{1}{2}\left(v_{ss} + \theta(v_s)^2\right)\sigma_{ss} + v_{\widehat{p}}\mu_{\widehat{p}} + \frac{1}{2}\left(v_{\widehat{p}\widehat{p}} + \theta(v_{\widehat{p}})^2\right)\sigma_{\widehat{p}\widehat{p}} \\ &+ (1-\gamma)v_s\sigma_{Cs} + (1-\gamma)v_{\widehat{p}}\sigma_{C\widehat{p}} + \left(v_{s\widehat{p}} + \theta v_s v_{\widehat{p}}\right)\sigma_{s\widehat{p}} \\ &+ \sum_{i=A,B}\frac{1}{\theta}\widehat{\lambda}_i\left[(1+s_iL_i)^{1-\gamma}e^{\theta v(s_A^{i+},\widehat{p}^{i+})-\theta v(s_A,\widehat{p})} - 1\right].\end{aligned} \tag{A.13}$$

For numerical tractability, we slightly reformulate this PDE. We apply the conjecture

$$J = \frac{C^{1-\gamma}}{1-\gamma}\beta^{\theta}\frac{g^{(K)}}{K}$$

for J, where $g^{(K)}$ is a twice differentiable function in both the output share s_A and the filtered probability $\widehat{p}$ and K is a positive constant. It relates to the log wealth-consumption via the equation $v = \frac{\ln\left(\frac{g^{(K)}}{K}\right)}{\theta}$. Plugging this guess for J into the aggregator function results in

$$f(C,J) = \theta J\left(\frac{\left(g^{(K)}\right)^{-\frac{1}{\theta}}}{K^{-\frac{1}{\theta}}} - \beta\right).$$

The infinitesimal generator DJ under the investor's filtration $\mathcal{G}$ again follows from Itô's Lemma:

$$\begin{aligned}\mathcal{D}J = {} & (1-\gamma)J\mu_C - \frac{1}{2}\gamma(1-\gamma)J\sigma_{CC} + \frac{g_s^{(K)}}{g^{(K)}}J\mu_s + \frac{1}{2}J\frac{g_{ss}^{(K)}}{g^{(K)}}\sigma_{ss} + \frac{g_{\widehat{p}}^{(K)}}{g^{(K)}}J\mu_{\widehat{p}} \\ & + \frac{1}{2}J\frac{g_{\widehat{p}\widehat{p}}^{(K)}}{g^{(K)}}\sigma_{\widehat{p}\widehat{p}} + (1-\gamma)J\frac{g_s^{(K)}}{g^{(K)}}\sigma_{Cs} + (1-\gamma)J\frac{g_{\widehat{p}}^{(K)}}{g^{(K)}}\sigma_{C\widehat{p}} + J\frac{g_{s\widehat{p}}^{(K)}}{g^{(K)}}\sigma_{s\widehat{p}} \\ & + \sum_{i=A,B}\widehat{\lambda}_i J\left[(1+s_iL_i)^{1-\gamma}\frac{g^{(K)}(s_A^{i+},\widehat{p}^{i+})}{g^{(K)}} - 1\right].\end{aligned}$$

Plugging these expressions into the Bellman equation, dividing by J and multiplying by $g^{(K)}$ gives

$$\begin{aligned}0 = {} & \theta\frac{\left(g^{(K)}\right)^{1-\frac{1}{\theta}}}{K^{-\frac{1}{\theta}}} - \theta\beta g^{(K)} + (1-\gamma)g^{(K)}\mu_C - \frac{1}{2}\gamma(1-\gamma)g^{(K)}\sigma_{CC} + g_s^{(K)}\mu_s + \frac{1}{2}g_{ss}^{(K)}\sigma_{ss} \\ & + g_{\widehat{p}}^{(K)}\mu_{\widehat{p}} + \frac{1}{2}g_{\widehat{p}\widehat{p}}^{(K)}\sigma_{\widehat{p}\widehat{p}} + (1-\gamma)g_s^{(K)}\sigma_{Cs} + (1-\gamma)g_{\widehat{p}}^{(K)}\sigma_{C\widehat{p}} + g_{s\widehat{p}}^{(K)}\sigma_{s\widehat{p}} \\ & + \sum_{i=A,B}\widehat{\lambda}_i\left[(1+s_iL_i)^{1-\gamma}g^{(K)}(s_A^{i+},\widehat{p}^{i+}) - g^{(K)}\right].\end{aligned}$$

After some rearranging of terms this PDE looks as follows

$$\begin{aligned}0 = {} & \theta\left(g^{(K)}\right)^{1-\frac{1}{\theta}}K^{\frac{1}{\theta}} + g^{(K)}\left[(1-\gamma)\mu_C - \frac{1}{2}\gamma(1-\gamma)\sigma_{CC} - \theta\beta\right] + g_s^{(K)}\left[\mu_s + (1-\gamma)\sigma_{Cs}\right] \\ & + g_{\widehat{p}}^{(K)}\left[\mu_{\widehat{p}} + (1-\gamma)\sigma_{C\widehat{p}}\right] + g_{ss}^{(K)}\frac{1}{2}\sigma_{ss} + g_{\widehat{p}\widehat{p}}^{(K)}\frac{1}{2}\sigma_{\widehat{p}\widehat{p}} + g_{s\widehat{p}}^{(K)}\sigma_{s\widehat{p}} \\ & + \sum_{i=A,B}\widehat{\lambda}_i\left[(1+s_iL_i)^{1-\gamma}g^{(K)}(s_A^{i+},\widehat{p}^{i+}) - g^{(K)}\right].\end{aligned}$$

We solve this PDE numerically. First of all, note that this PDE is (approximately) elliptic. Elliptic PDEs usually require boundary conditions on the whole boundary of the domain where the equation is supposed to be solved (compare e.g. the classical Dirichlet problem). The solution of the Dirichlet problem is typically unique and in the interior of the domain as smooth as the coefficients of the elliptic operator. In contrast, our equation is given without any boundary conditions. A natural way to obtain boundary conditions would be to let the output share s_A and the state variable $\widehat{p}$ tend to 0 or 1 and solve the

respective equilibria. However, the economies on these boundaries are structurally different from our economy, e.g. they involve one Lucas tree instead of two. It is thus not self-evident that the solution in our two-tree economy should converge to the corresponding one-tree solutions.

We do not take a stand on this point here. Oleinik and Radkevich (1973) show that certain elliptic equations have unique weak solutions even without boundary conditions. Two definitions are needed for this uniqueness theorem. A PDE is called degenerate at a point on the boundary if the principal part of the PDE vanishes at this point. A boundary problem is called Keldys-Fichera boundary problem, if parts of the (potential) boundary are such that there is no positive drift in the direction of the outward normal vector. If additionally some usual Caratheodory and growth conditions for the coefficients hold (such that existence of a solution is guaranteed), Oleinik and Radkevich (1973) show that it is not necessary to impose boundary conditions on those parts of the boundary where a linear elliptic operator becomes degenerate and the Keldys-Fichera drift condition holds. Based on this theory, Ma and Yu (1989) prove the existence and uniqueness of weak solutions of a certain type of quasilinear degenerate Keldys-Fichera boundary problems. If we disregard the nonlocal jump terms for a minute, our PDE satisfies exactly the required conditions: our elliptic operator is quasilinear (i.e. nonlinear with linear principal part), it becomes degenerate on the boundary and there is no positive drift in the outward normal direction of the domain $[0,1] \times [0,1]$ at any point of the boundary. The nonlocal terms do not change this behavior of the function v in general because the jump size is zero on the boundary anyway. The paper of Ma and Yu (1989) thus ensures existence and uniqueness of a weak solution of our PDE.[20] A similar case (although in a different economic context) is analyzed by Pakos (2012). A detailed summary of the theory of degenerate elliptic operators is also given in the book of Oleinik and Radkevich (1973).

Given the difficulties concerning the boundaries, we solve the PDE for $g^{(K)}(s_A, \widehat{p})$ numerically on a subset of $[0,1] \times [0,1]$ without boundary conditions using finite differences. Since the solution does not depend on any boundary conditions, it is not clear that the function v converges to the values which we could be tempted to assign on the boundaries using economic thinking. Possible boundary conditions in s_A would be the corresponding one-tree economies, boundary conditions in $\widehat{p}$ would be economies where the agent is totally sure to be in one of the two states. Whether the solution v has a continuous (or even differentiable) continuation on $[0,1] \times [0,1]$ is unclear. We leave this question open for future research.

A.3 Price-Dividend Ratios of Dividend Claims

Under the filtration $\mathcal{G}$, the dividends follow

$$\frac{dD_{i,t}}{D_{i,t-}} = \left(\phi\widehat{\mu}_{i,t} + \frac{1}{2}\phi(\phi-1)\sigma_i^2\right)dt + \phi\sigma_i d\widetilde{W}_{i,t} + ((1+L_i)^{\phi}-1)d\widehat{N}_{i,t},$$

[20] A weak solution is by definition an element of the Sobolev space $W^{k,p}$, i.e. a function in $L^p(\Omega)$ whose weak derivatives up to order k are also in $L^p(\Omega)$. In our case, Ma and Yu (1989) show that the unique solution is an element the Sobolev space $W^{1,2}$. In particular, by the Sobolev embedding theorem, it is thus continuous up to a set of measure zero.

for $i \in \{A, B\}$. Let ω_A denote the log price-dividend ratio of asset A. For $g(\xi, D_A, \omega_A) = \xi D_A e^{\omega_A}$, the Feynman-Kac formula yields

$$\frac{Dg(\xi, D_A, \omega_A)}{g(\xi, D_A, \omega_A)} + e^{-\omega_A} = 0. \tag{A.14}$$

Itô's Lemma gives

$$\frac{Dg}{g} = \mu_\xi + \phi\widehat{\mu}_A + \frac{1}{2}\phi(\phi-1)\sigma_A^2 + \mu_\omega + \frac{1}{2}\frac{d[\omega_A^c]}{dt} + \frac{d\langle \xi^c, D_A^c\rangle}{\xi D_A dt} + \frac{d\langle \omega_A^c, D_A^c\rangle}{D_A dt} + \frac{d\langle \omega_A^c, \xi^c\rangle}{\xi dt} + \text{Jump Terms.}$$

Another application of Itô's Lemma leads to

$$\begin{aligned}
d\omega_A = &\left[\omega_{A,s}\mu_s + \frac{1}{2}\omega_{A,ss}\sigma_{ss} + \omega_{A,\widehat{p}}\mu_{\widehat{p}} + \frac{1}{2}\omega_{A,\widehat{p}\widehat{p}}\sigma_{\widehat{p}\widehat{p}} + \omega_{A,s\widehat{p}}\sigma_{s\widehat{p}}\right]dt \\
&+ \left[\omega_{A,s}s_A s_B\sigma_A + \omega_{A,\widehat{p}}\widehat{p}(1-\widehat{p})\left(\frac{(\mu_A^{calm}-\mu_A^{cont})}{(1-\rho^2)\sigma_A} - \frac{\rho(\mu_B^{calm}-\mu_B^{cont})}{(1-\rho^2)\sigma_B}\right)\right]d\widehat{W}_{A,t} \\
&+ \left[-\omega_{A,s}s_A s_B\sigma_B + \omega_{A,\widehat{p}}\widehat{p}(1-\widehat{p})\left(\frac{(\mu_B^{calm}-\mu_B^{cont})}{(1-\rho^2)\sigma_B} - \frac{\rho(\mu_A^{calm}-\mu_A^{cont})}{(1-\rho^2)\sigma_A}\right)\right]d\widehat{W}_{B,t} \\
&+ (\omega_A(s_A^{A+}, \widehat{p}^{A+}) - \omega_A(s_A, \widehat{p}))d\widehat{N}_A + (\omega_A(s_A^{B+}, \widehat{p}^{B+}) - \omega_A(s_A, \widehat{p}))d\widehat{N}_B,
\end{aligned}$$

where, again, the subscripts s, $\widehat{p}$, ss, $\widehat{p}\widehat{p}$ and $s\widehat{p}$ denote the first and second derivatives with respect to state variables s_A and $\widehat{p}$. Plugging everything into equation $(A.14)$ and simplifying leads to the following PDE for ω_A:

$$\begin{aligned}
0 = &\, e^{-\omega_A} + \mu_\xi + \phi\widehat{\mu}_A + \frac{1}{2}\phi(\phi-1)\sigma_A^2 + \omega_{A,s}\mu_s + \frac{1}{2}\left(\omega_{A,ss} + \omega_{A,s}^2\right)\sigma_{ss} \\
&+ \omega_{A,\widehat{p}}\mu_{\widehat{p}} + \frac{1}{2}\left(\omega_{A,\widehat{p}\widehat{p}} + \omega_{A,\widehat{p}}^2\right)\sigma_{\widehat{p}\widehat{p}} + \omega_{A,s}s_A s_B\phi\sigma_A^2 - \omega_{A,s}s_A s_B\phi\rho\sigma_A\sigma_B \\
&+ \left(\omega_{A,s\widehat{p}} + \omega_{A,s}\omega_{A,\widehat{p}}\right)\sigma_{s\widehat{p}} + \omega_{A,\widehat{p}}\widehat{p}(1-\widehat{p})(\mu_A^{calm}-\mu_A^{cont})\phi \\
&- \eta_A^{diff}\left(\phi\sigma_A + \omega_{A,s}s_A s_B\sigma_A - \omega_{A,s}s_A s_B\rho\sigma_B + \omega_{A,\widehat{p}}\widehat{p}(1-\widehat{p})\frac{(\mu_A^{calm}-\mu_A^{cont})}{\sigma_A}\right) \\
&- \eta_B^{diff}\left(\phi\rho\sigma_A - \omega_{A,s}s_A s_B\sigma_B + \omega_{A,s}s_A s_B\rho\sigma_A + \omega_{A,\widehat{p}}\widehat{p}(1-\widehat{p})\frac{(\mu_B^{calm}-\mu_B^{cont})}{\sigma_B}\right) \\
&+ \widehat{\lambda}_A\left[(1+\eta_A^{jump})(1+L_A)^\phi e^{\omega_A(s_A^{A+}, \widehat{p}^{A+}) - \omega_A(s_A,\widehat{p})} - 1\right] \\
&+ \widehat{\lambda}_B\left[(1+\eta_B^{jump})e^{\omega_A(s_A^{B+}, \widehat{p}^{B+}) - \omega_A(s_A,\widehat{p})} - 1\right].
\end{aligned} \tag{A.15}$$

For numerical reasons, we solve a transformed version of this PDE again. We define $h_A = e^{\omega_A}$ and multiply the PDE (A.15) by h_A. Again, the subscripts s, $\widehat{p}$, ss, $\widehat{p}\widehat{p}$ and $s\widehat{p}$ denote the first and second derivatives with respect to s_A and $\widehat{p}$. This leads to the following PDE for h_A:

$$\begin{aligned}
0 = &\, 1 + h_A\mu_\xi + h_A\phi\widehat{\mu}_A + h_A\frac{1}{2}\phi(\phi-1)\sigma_A^2 + h_{A,s}\mu_s + \frac{1}{2}h_{A,ss}\sigma_{ss} \\
&+ h_{A,\widehat{p}}\mu_{\widehat{p}} + \frac{1}{2}h_{A,\widehat{p}\widehat{p}}\sigma_{\widehat{p}\widehat{p}} + h_{A,s}s_A s_B\phi\sigma_A^2 - h_{A,s}s_A s_B\phi\rho\sigma_A\sigma_B \\
&+ h_{A,s\widehat{p}}\sigma_{s\widehat{p}} + h_{A,\widehat{p}}\widehat{p}(1-\widehat{p})(\mu_A^{calm}-\mu_A^{cont})\phi \\
&- \eta_A^{diff}\left(h_A\phi\sigma_A + h_{A,s}s_A s_B\sigma_A - h_{A,s}s_A s_B\rho\sigma_B + h_{A,\widehat{p}}\widehat{p}(1-\widehat{p})\frac{(\mu_A^{calm}-\mu_A^{cont})}{\sigma_A}\right)
\end{aligned} \tag{A.16}$$

$$
\begin{aligned}
&- \eta_B^{diff}\left(h_A\phi\rho\sigma_A - h_{A,s}s_As_B\sigma_B + h_{A,s}s_As_B\rho\sigma_A + h_{A,\widehat{p}}\widehat{p}(1-\widehat{p})\frac{(\mu_B^{calm}-\mu_B^{cont})}{\sigma_B}\right)\\
&+ \widehat{\lambda}_A\left[(1+\eta_A^{jump})(1+L_A)^{\phi}h_A(s_A^{A+},\widehat{p}^{A+}) - h_A(s_A,\widehat{p})\right]\\
&+ \widehat{\lambda}_B\left[(1+\eta_B^{jump})h_A(s_A^{B+},\widehat{p}^{B+}) - h_A(s_A,\widehat{p})\right].
\end{aligned}
$$

The log price-dividend ratio ω_B satisfies an analogous PDE. Note that a similar argument as for wealth-consumption ratio holds concerning potential boundary conditions for this PDE.

A.4 Pricing Kernel, Market Prices of Risk and Risk-Free Rate

We derive the dynamics of the pricing kernel from the Duffie and Epstein (1992a) result (8), the dynamics of C in (7) and the following dynamics of v derived via Itô's Lemma:

$$
\begin{aligned}
dv = &\left[v_s\mu_s + \frac{1}{2}v_{ss}\sigma_{ss} + v_{\widehat{p}}\mu_{\widehat{p}} + \frac{1}{2}v_{\widehat{p}\widehat{p}}\sigma_{\widehat{p}\widehat{p}} + v_{s\widehat{p}}\sigma_{s\widehat{p}}\right]dt + v_ss_As_B\left(\sigma_A d\widehat{W}_{A,t} - \sigma_B d\widehat{W}_{B,t}\right)\\
&+ v_p\widehat{p}(1-\widehat{p})\left(\frac{(\mu_A^{calm}-\mu_A^{cont})}{(1-\rho^2)\sigma_A} - \frac{\rho(\mu_B^{calm}-\mu_B^{cont})}{(1-\rho^2)\sigma_B}\right)d\widehat{W}_{A,t}\\
&+ v_p\widehat{p}(1-\widehat{p})\left(\frac{(\mu_B^{calm}-\mu_B^{cont})}{(1-\rho^2)\sigma_B} - \frac{\rho(\mu_A^{calm}-\mu_A^{cont})}{(1-\rho^2)\sigma_A}\right)d\widehat{W}_{B,t}\\
&+ \text{Jump Terms}.
\end{aligned}
$$

The shortcuts $\mu_s, \sigma_{ss}, \mu_{\widehat{p}}, \sigma_{\widehat{p}\widehat{p}}$ and $\sigma_{s\widehat{p}}$ are defined in $(A.6), (A.7), (A.8), (A.9)$ and $(A.12)$. This implies

$$
\begin{aligned}
\frac{d\xi_t}{\xi_{t-}} = &\left(-\beta\theta + (\theta-1)e^{-v_t}\right)dt - \gamma\mu_C dt + (\theta-1)v_s\mu_s dt\\
&- (\theta-1)v_s\gamma\sigma_{Cs}dt + \frac{1}{2}(\theta-1)\left(v_{ss} + (\theta-1)(v_s)^2\right)\sigma_{ss}dt\\
&+ \frac{1}{2}\gamma(1+\gamma)\sigma_{CC}dt + (\theta-1)v_{\widehat{p}}\mu_{\widehat{p}}dt - (\theta-1)v_{\widehat{p}}\gamma\sigma_{C\widehat{p}}dt\\
&+ \frac{1}{2}(\theta-1)\left(v_{\widehat{p}\widehat{p}} + (\theta-1)(v_{\widehat{p}})^2\right)\sigma_{\widehat{p}\widehat{p}}dt + (\theta-1)\left(v_{s\widehat{p}} + (\theta-1)v_sv_{\widehat{p}}\right)\sigma_{s\widehat{p}}dt\\
&- \eta_A^{diff}d\widehat{W}_{A,t} - \eta_B^{diff}d\widehat{W}_{B,t} + \eta_A^{jump}d\widehat{N}_{A,t} + \eta_B^{jump}d\widehat{N}_{B,t},
\end{aligned}
$$

where additionally $\mu_C, \sigma_{CC}, \sigma_{Cp}$ and σ_{Cs} are defined in $(A.4), (A.5), (A.11)$ and $(A.10)$. The market prices of risk for diffusive risk are given by

$$
\begin{aligned}
\eta_A^{diff} &= \gamma s_A\sigma_A - (\theta-1)v_ss_As_B\sigma_A - (\theta-1)v_{\widehat{p}}\widehat{p}(1-\widehat{p})\left(\frac{(\mu_A^{calm}-\mu_A^{cont})}{(1-\rho^2)\sigma_A} - \frac{\rho(\mu_B^{calm}-\mu_B^{cont})}{(1-\rho^2)\sigma_B}\right)\\
\eta_B^{diff} &= \gamma s_B\sigma_B + (\theta-1)v_ss_As_B\sigma_B - (\theta-1)v_{\widehat{p}}\widehat{p}(1-\widehat{p})\left(\frac{(\mu_B^{calm}-\mu_B^{cont})}{(1-\rho^2)\sigma_B} - \frac{\rho(\mu_A^{calm}-\mu_A^{cont})}{(1-\rho^2)\sigma_A}\right).
\end{aligned}
$$

The market prices for jump risk are equal to

$$
\begin{aligned}
\eta_A^{jump} &= (1+s_AL_A)^{-\gamma}e^{(\theta-1)\left(v(s_A^{A+},\widehat{p}^{A+}) - v(s_A,\widehat{p})\right)} - 1\\
\eta_B^{jump} &= (1+s_BL_B)^{-\gamma}e^{(\theta-1)\left(v(s_A^{B+},\widehat{p}^{B+}) - v(s_A,\widehat{p})\right)} - 1.
\end{aligned}
$$

Note that regime switches from the contagion state back to the calm state are not priced. These regime switches do not have any impact on observable state variables ($\widehat{p}$ and s_A). The risk-neutral jump intensities have the form $\widehat{\lambda}_i^{\mathbb{Q}} = \widehat{\lambda}_i^{\mathbb{P}}(1+\eta_i^{jump})$. For future use we abbreviate the drift rate of the pricing kernel as

$$\begin{aligned}\mu_\xi = &-\beta\theta + (\theta-1)e^{-v} - \gamma\mu_C + (\theta-1)v_s\mu_s - (\theta-1)v_s\gamma\sigma_{Cs} \\ &+ \frac{1}{2}(\theta-1)\left(v_{ss} + (\theta-1)(v_s)^2\right)\sigma_{ss} + \frac{1}{2}\gamma(1+\gamma)\sigma_{CC} + (\theta-1)v_{\widehat{p}}\mu_{\widehat{p}} - (\theta-1)v_{\widehat{p}}\gamma\sigma_{C\widehat{p}} \\ &+ \frac{1}{2}(\theta-1)\left(v_{\widehat{p}\widehat{p}} + (\theta-1)(v_{\widehat{p}})^2\right)\sigma_{\widehat{p}\widehat{p}} + (\theta-1)\left(v_{s\widehat{p}} + (\theta-1)v_s v_{\widehat{p}}\right)\sigma_{s\widehat{p}}.\end{aligned}$$

Using the PDE ($A.13$) for v, we can rewrite the drift of the pricing kernel as follows

$$\begin{aligned}\mu_\xi = &-\beta - \frac{1}{\psi}\mu_C + \frac{1}{2}\gamma\left(1+\frac{1}{\psi}\right)\sigma_{CC} + (1-\theta)v_s\sigma_{Cs} + (1-\theta)v_{\widehat{p}}\sigma_{C\widehat{p}} \\ &+ \frac{1}{2}(1-\theta)v_s^2\sigma_{ss} + \frac{1}{2}(1-\theta)v_{\widehat{p}}^2\sigma_{\widehat{p}\widehat{p}} + (1-\theta)v_s v_{\widehat{p}}\sigma_{s\widehat{p}} \\ &- \frac{\theta-1}{\theta}\widehat{\lambda}_A\left[(1+s_A L_A)^{1-\gamma}e^{\theta\left(v(s_A^{A+},\widehat{p}^{A+})-v(s_A,\widehat{p})\right)} - 1\right] \\ &- \frac{\theta-1}{\theta}\widehat{\lambda}_B\left[(1+s_B L_B)^{1-\gamma}e^{\theta\left(v(s_A^{B+},\widehat{p}^{B+})-v(s_A,\widehat{p})\right)} - 1\right].\end{aligned}$$

The risk-free rate in the economy is given by

$$r_f = -\mu_\xi - \widehat{\lambda}_A\eta_A^{jump} - \widehat{\lambda}_B\eta_B^{jump},$$

and thus by plugging in μ_ξ we obtain

$$\begin{aligned}r_f = &\beta + \frac{1}{\psi}\mu_C - \frac{1}{2}\gamma\left(1+\frac{1}{\psi}\right)\sigma_{CC} - (1-\theta)v_s\sigma_{Cs} - (1-\theta)v_{\widehat{p}}\sigma_{C\widehat{p}} \\ &- \frac{1}{2}(1-\theta)v_s^2\sigma_{ss} - \frac{1}{2}(1-\theta)v_{\widehat{p}}^2\sigma_{\widehat{p}\widehat{p}} - (1-\theta)v_s v_{\widehat{p}}\sigma_{s\widehat{p}} \\ &- \sum_{i=A,B}\widehat{\lambda}_i\left[\eta_i^{jump} + \frac{1-\theta}{\theta}\left((1+s_i L_i)^{1-\gamma}e^{\theta\left(v(s_A^{i+},\widehat{p}^{i+})-v(s_A,\widehat{p})\right)} - 1\right)\right].\end{aligned}$$

A.5 Expected Returns, Volatilities and Correlations

The dynamics of the asset price $P_A = e^{\omega_A}D_A$ follow via Itô's Lemma. We obtain

$$\begin{aligned}\frac{dP_{A,t}}{P_{A,t-}} = &\frac{E_t[dP_{A,t}]}{P_{A,t-}} + \Upsilon_A^{A,jump}d\widehat{N}_{A,t} + \Upsilon_A^{B,jump}d\widehat{N}_{B,t} \\ &+ \left(\omega_{A,s}s_{A,t}s_{B,t}\sigma_A + \omega_{A,\widehat{p}}\widehat{p}_t(1-\widehat{p}_t)\left(\frac{(\mu_A^{calm}-\mu_A^{cont})}{(1-\rho^2)\sigma_A} - \frac{(\mu_B^{calm}-\mu_B^{cont})\rho}{(1-\rho^2)\sigma_B}\right) + \phi\sigma_A\right)d\widehat{W}_{A,t} \\ &+ \left(\omega_{A,\widehat{p}}\widehat{p}_t(1-\widehat{p}_t)\left(\frac{(\mu_B^{calm}-\mu_B^{cont})}{(1-\rho^2)\sigma_B} - \frac{(\mu_A^{calm}-\mu_A^{cont})\rho}{(1-\rho^2)\sigma_A}\right) - \omega_{A,s}s_{A,t}s_{B,t}\sigma_B\right)d\widehat{W}_{B,t}.\end{aligned}$$

In the following, we set

$$\Upsilon_A^{A,diff} = (\omega_{A,s} s_A s_B + \phi)\,\sigma_A - \omega_{A,s} s_A s_B \sigma_B \rho + \omega_{A,\widehat{p}} \widehat{p}(1-\widehat{p}) \left(\frac{(\mu_A^{calm} - \mu_A^{cont})}{\sigma_A} \right)$$
$$\Upsilon_A^{B,diff} = (\omega_{A,s} s_A s_B + \phi)\,\rho\sigma_A - \omega_{A,s} s_A s_B \sigma_B + \omega_{A,\widehat{p}} \widehat{p}(1-\widehat{p}) \left(\frac{(\mu_B^{calm} - \mu_B^{cont})}{\sigma_B} \right),$$

which can be interpreted as the total sensitivities of asset A with respect to the Brownian shocks $\widehat{W}_A$ and $\widehat{W}_B$. The total sensitivities $\Upsilon_B^{A,diff}$ and $\Upsilon_B^{B,diff}$ are defined analogously. The sensitivities of asset A with respect to the jump processes are

$$\begin{aligned}
\Upsilon_A^{A,jump} &= (1+L_A)^{\phi} e^{\omega_A(s_A^{A+}, \widehat{p}^{A+}) - \omega_A(s_A, \widehat{p})} - 1 \\
\Upsilon_A^{B,jump} &= e^{\omega_A(s_A^{B+}, \widehat{p}^{B+}) - \omega_A(s_A, \widehat{p})} - 1 \\
\Upsilon_A^{cont,calm} &= 0.
\end{aligned}$$

For the exposures of asset B, one has to switch 'A' and 'B' on both sides of the equations and replace every derivative ω_s by $\omega_{1-s} = -\omega_s$. The expected return of asset A can be computed as the sum of expected price change and dividend yield:

$$\frac{E_t[dR_{A,t}]}{dt} = \frac{E_t[dP_{A,t}]}{P_{A,t}dt} + e^{-\omega_{A,t}}.$$

Replacing $e^{-\omega_A}$ using the differential equation $(A.15)$, computing the expectation of dP_A, rearranging some terms and finally using the expression for the risk-free rate or alternatively multiplying exposures with the appropiate market prices of risk, the expected excess return of asset A becomes

$$\begin{aligned}
&\Upsilon_A^{A,diff}\eta_A^{diff} + \Upsilon_A^{B,diff}\eta_B^{diff} - \widehat{\lambda}_A \Upsilon_A^{A,jump}\eta_A^{jump} - \widehat{\lambda}_B \Upsilon_A^{B,jump}\eta_B^{jump} \\
&= \left\{ (\omega_{A,s} s_A s_B + \phi)\,\sigma_A - \omega_{A,s} s_A s_B \sigma_B \rho + \omega_{A,\widehat{p}} \widehat{p}(1-\widehat{p}) \left(\frac{(\mu_A^{calm} - \mu_A^{cont})}{\sigma_A} \right) \right\} \\
&\quad \cdot \left\{ \gamma s_A \sigma_A - (\theta-1) v_s s_A s_B \sigma_A - (\theta-1) v_{\widehat{p}} \widehat{p}(1-\widehat{p}) \left(\frac{(\mu_A^{calm} - \mu_A^{cont})}{(1-\rho^2)\sigma_A} - \frac{\rho(\mu_B^{calm} - \mu_B^{cont})}{(1-\rho^2)\sigma_B} \right) \right\} \\
&\quad + \left\{ (\omega_{A,s} s_A s_B + \phi)\,\rho\sigma_A - \omega_{A,s} s_A s_B \sigma_B + \omega_{A,\widehat{p}} \widehat{p}(1-\widehat{p}) \left(\frac{(\mu_B^{calm} - \mu_B^{cont})}{\sigma_B} \right) \right\} \\
&\quad \cdot \left\{ \gamma s_B \sigma_B + (\theta-1) v_s s_A s_B \sigma_B - (\theta-1) v_{\widehat{p}} \widehat{p}(1-\widehat{p}) \left(\frac{(\mu_B^{calm} - \mu_B^{cont})}{(1-\rho^2)\sigma_B} - \frac{\rho(\mu_A^{calm} - \mu_A^{cont})}{(1-\rho^2)\sigma_A} \right) \right\} \\
&\quad + \widehat{\lambda}_A \left[(1+L_A)^{\phi} e^{\omega_A(s_A^{A+}, \widehat{p}^{A+}) - \omega_A(s_A, \widehat{p})} - 1 \right] \left[1 - (1+s_A L_A)^{-\gamma} e^{(\theta-1)\left(v(s_A^{A+}, \widehat{p}^{A+}) - v(s_A, \widehat{p})\right)} \right] \\
&\quad + \widehat{\lambda}_B \left[e^{\omega_A(s_A^{B+}, \widehat{p}^{B+}) - \omega_A(s_A, \widehat{p})} - 1 \right] \left[1 - (1+s_B L_B)^{-\gamma} e^{(\theta-1)\left(v(s_A^{B+}, \widehat{p}^{B+}) - v(s_A, \widehat{p})\right)} \right].
\end{aligned}$$

The local variance of asset A follows directly from the asset price dynamics:

$$\begin{aligned}\frac{d\langle P_A\rangle_t}{(P_{A,t})^2}\frac{1}{dt} = &\left(\omega_{A,s}s_{A,t}s_{B,t}\sigma_A + \omega_{A,\widehat{p}}\widehat{p}_t(1-\widehat{p}_t)\left(\frac{(\mu_A^{calm}-\mu_A^{cont})}{(1-\rho^2)\sigma_A} - \frac{(\mu_B^{calm}-\mu_B^{cont})\rho}{(1-\rho^2)\sigma_B}\right) + \phi\sigma_A\right)^2 \\ &+ \left(\omega_{A,\widehat{p}}\widehat{p}_t(1-\widehat{p}_t)\left(\frac{(\mu_B^{calm}-\mu_B^{cont})}{(1-\rho^2)\sigma_B} - \frac{(\mu_A^{calm}-\mu_A^{cont})\rho}{(1-\rho^2)\sigma_A}\right) - \omega_{A,s}s_{A,t}s_{B,t}\sigma_B\right)^2 \\ &+ 2\rho\left(\omega_{A,s}s_{A,t}s_{B,t}\sigma_A + \omega_{A,\widehat{p}}\widehat{p}_t(1-\widehat{p}_t)\left(\frac{(\mu_A^{calm}-\mu_A^{cont})}{(1-\rho^2)\sigma_A} - \frac{(\mu_B^{calm}-\mu_B^{cont})\rho}{(1-\rho^2)\sigma_B}\right) + \phi\sigma_A\right) \\ &\quad\cdot\left(\omega_{A,\widehat{p}}\widehat{p}_t(1-\widehat{p}_t)\left(\frac{(\mu_B^{calm}-\mu_B^{cont})}{(1-\rho^2)\sigma_B} - \frac{(\mu_A^{calm}-\mu_A^{cont})\rho}{(1-\rho^2)\sigma_A}\right) - \omega_{A,s}s_{A,t}s_{B,t}\sigma_B\right) \\ &+ \widehat{\lambda}_A\left(\Upsilon_A^{A,jump}\right)^2 + \widehat{\lambda}_B\left(\Upsilon_A^{B,jump}\right)^2.\end{aligned}$$

The local correlation between the prices of asset A and B is given by

$$Corr_{A,B,t} = \frac{d\langle P_A, P_B\rangle_t}{\sqrt{d\langle P_A\rangle_t\, d\langle P_B\rangle_t}}.$$

The local variance of asset B and the local covariance can be computed from the price dynamics of asset B which are completely symmetric to the dynamics of asset A. The local covariance is given by

$$\begin{aligned}\frac{d\langle P_A, P_B\rangle_t}{P_{A,t}P_{B,t}}\frac{1}{dt} = &\rho\left(\omega_{A,s}s_{A,t}s_{B,t}\sigma_A + \omega_{A,\widehat{p}}\widehat{p}_t(1-\widehat{p}_t)\left(\frac{(\mu_A^{calm}-\mu_A^{cont})}{(1-\rho^2)\sigma_A} - \frac{(\mu_B^{calm}-\mu_B^{cont})\rho}{(1-\rho^2)\sigma_B}\right) + \phi\sigma_A\right) \\ &\cdot\left(-\omega_{B,s}s_{A,t}s_{B,t}\sigma_B + \omega_{B,\widehat{p}}\widehat{p}_t(1-\widehat{p}_t)\left(\frac{(\mu_B^{calm}-\mu_B^{cont})}{(1-\rho^2)\sigma_B} - \frac{(\mu_A^{calm}-\mu_A^{cont})\rho}{(1-\rho^2)\sigma_A}\right) + \phi\sigma_B\right) \\ &+ \rho\left(\omega_{A,\widehat{p}}\widehat{p}_t(1-\widehat{p}_t)\left(\frac{(\mu_B^{calm}-\mu_B^{cont})}{(1-\rho^2)\sigma_B} - \frac{(\mu_A^{calm}-\mu_A^{cont})\rho}{(1-\rho^2)\sigma_A}\right) - \omega_{A,s}s_{A,t}s_{B,t}\sigma_B\right) \\ &\cdot\left(\omega_{B,\widehat{p}}\widehat{p}_t(1-\widehat{p}_t)\left(\frac{(\mu_A^{calm}-\mu_A^{cont})}{(1-\rho^2)\sigma_A} - \frac{(\mu_B^{calm}-\mu_B^{cont})\rho}{(1-\rho^2)\sigma_B}\right) + \omega_{B,s}s_{A,t}s_{B,t}\sigma_A\right) \\ &+ \left(\omega_{A,s}s_{A,t}s_{B,t}\sigma_A + \omega_{A,\widehat{p}}\widehat{p}_t(1-\widehat{p}_t)\left(\frac{(\mu_A^{calm}-\mu_A^{cont})}{\sigma_A} - \frac{(\mu_B^{calm}-\mu_B^{cont})\rho}{\sigma_B}\right) + \phi\sigma_A\right) \\ &\quad\cdot\left(\omega_{B,\widehat{p}}\widehat{p}_t(1-\widehat{p}_t)\left(\frac{(\mu_A^{calm}-\mu_A^{cont})}{\sigma_A} - \frac{(\mu_B^{calm}-\mu_B^{cont})\rho}{\sigma_B}\right) + \omega_{B,s}s_{A,t}s_{B,t}\sigma_A\right) \\ &+ \left(-\omega_{B,s}s_{A,t}s_{B,t}\sigma_B + \omega_{B,\widehat{p}}\widehat{p}_t(1-\widehat{p}_t)\left(\frac{(\mu_B^{calm}-\mu_B^{cont})}{(1-\rho^2)\sigma_B} - \frac{(\mu_A^{calm}-\mu_A^{cont})\rho}{(1-\rho^2)\sigma_A}\right) + \phi\sigma_B\right) \\ &\quad\cdot\left(\omega_{A,\widehat{p}}\widehat{p}_t(1-\widehat{p}_t)\left(\frac{(\mu_B^{calm}-\mu_B^{cont})}{(1-\rho^2)\sigma_B} - \frac{(\mu_A^{calm}-\mu_A^{cont})\rho}{(1-\rho^2)\sigma_A}\right) - \omega_{A,s}s_{A,t}s_{B,t}\sigma_B\right) \\ &+ \widehat{\lambda}_A\Upsilon_A^{A,jump}\Upsilon_B^{A,jump} + \widehat{\lambda}_B\Upsilon_A^{B,jump}\Upsilon_B^{B,jump}.\end{aligned}$$

A.6 Dividend Strips

The following definitions are taken from Belo, Collin-Dufresne, and Goldstein (2012). A dividend strip is a claim on the value of the dividend at time T. Thus, its value at time t is given by

$$V_A^T(t) = E_t^{\mathbb{Q}}\left[e^{-r_f(T-t)}D_{A,T}\right] = E_t\left[\xi_{t,T}D_{A,T}\right],$$

where we have

$$D_{A,T} = D_{A,t} \exp\left[\left(\phi\widehat{\mu}_{A,t} + \frac{1}{2}\phi(\phi-1)\sigma_A^2 - \frac{1}{2}\phi^2\sigma_A^2\right)(T-t) \right. \\ \left. + \phi\sigma_A\left(\widehat{W}_{A,T} - \widehat{W}_{A,t}\right) + \log((1+L_A)^\phi - 1)\left(\widehat{N}_{A,T} - \widehat{N}_{A,t}\right)\right],$$

and

$$\xi_{t,T} = \beta^\theta \left(\frac{C_T}{C_t}\right)^{-\gamma} e^{-\beta\theta(T-t)+(\theta-1)\left(\int_t^T e^{-v(s_u,\widehat{p}_u)}du + v(s_T,\widehat{p}_T)\right)}.$$

Define $y_{A,t} = \log\frac{V_A^T(t)}{D_{A,t}}$. The Feynman-Kac formula applied to $i(\xi_t, y_t, D_{A,t}) = \xi_t D_{A,t} e^{y_{A,t}} = E_t[\xi_T D_{A,T}]$ yields the following partial differential equation

$$\begin{aligned} 0 &= \mathcal{D}i \\ &= \frac{\partial i}{\partial t}dt + \frac{\partial i}{\partial \xi_t}d\xi_t + \frac{\partial i}{\partial y_{A,t}}dy_{A,t} + \frac{\partial i}{\partial D_{A,t}}dD_{A,t} + \frac{1}{2}\frac{\partial^2 i}{\partial \xi_t^2}d\langle\xi_t\rangle + \frac{1}{2}\frac{\partial^2 i}{\partial D_{A,t}^2}d\langle D_{A,t}\rangle \\ &\quad + \frac{1}{2}\frac{\partial^2 i}{\partial y_{A,t}^2}d\langle y_{A,t}\rangle + \frac{\partial^2 i}{\partial \xi_t \partial D_{A,t}}d\langle\xi_t, D_{A,t}\rangle + \frac{\partial^2 i}{\partial \xi_t \partial y_{A,t}}d\langle\xi_t, y_{A,t}\rangle + \frac{\partial^2 i}{\partial D_{A,t}\partial y_{A,t}}d\langle D_{A,t}, y_{A,t}\rangle \\ &\quad + \sum_{j=A,B}\widehat{\lambda}_{j,t}\left(\xi_t^{j+}D_{A,t}^{j+}e^{y_{A,t}^{j+}} - \xi_t D_{A,t}e^{y_{A,t}}\right). \end{aligned} \tag{A.17}$$

with boundary condition $i(\xi_T, y_T, D_{A,T}) = \xi_T D_{A,T}$ which is equivalent to $e^{y_{A,T}} = 1$. Note that $\frac{\partial i}{\partial t}$ is zero. Using the functional form of i we thus obtain

$$\begin{aligned} 0 &= i\cdot\frac{d\xi_t}{\xi_t} + i\cdot dy_{A,t} + i\cdot\frac{dD_{A,t}}{D_{A,t}} + i\cdot\frac{1}{2}d\langle y_{A,t}\rangle \\ &\quad + i\cdot\frac{d\langle\xi_t, D_{A,t}\rangle}{\xi_t D_{A,t}} + i\cdot\frac{d\langle\xi_t, y_{A,t}\rangle}{\xi_t} + i\cdot\frac{d\langle D_{A,t}, y_{A,t}\rangle}{D_{A,t}} \\ &\quad + i\cdot\sum_{j=A,B}\widehat{\lambda}_{j,t}\left((1+\eta_j^{jump})(1+L_j)^\phi e^{y_A(s_A^{j+},\widehat{p}^{j+}) - y_A(s_A,\widehat{p})} - 1\right). \end{aligned} \tag{A.18}$$

We divide this PDE by i. The dynamics of ξ_t and $D_{A,t}$ have been given above. The dynamics of $y_{A,t}$ follow from an application of Itô's Lemma and have the same form as the dynamics of the log price-dividend ratio ω_A except that the dynamics of $y_{A,t}$ now also include a time derivative. Altogether, the function y_A satisfies a PDE similar to the PDE for the log price-dividend ratio w_A except for the time derivative $\frac{\partial y_{A,t}}{\partial t} \neq 0$. The dynamics of $y_{A,t}$ follow from Itô's Lemma:

$$\begin{aligned} dy_A &= \left[\frac{\partial y_A}{\partial t} + y_{A,s}\mu_s + \frac{1}{2}y_{A,ss}\sigma_{ss} + y_{A,\widehat{p}}\mu_{\widehat{p}} + \frac{1}{2}y_{A,\widehat{p}\widehat{p}}\sigma_{\widehat{p}\widehat{p}} + y_{A,s\widehat{p}}\sigma_{s\widehat{p}}\right]dt \\ &\quad + \left[y_{A,s}s_A s_B\sigma_A + y_{A,\widehat{p}}\widehat{p}(1-\widehat{p})\left(\frac{(\mu_A^{calm} - \mu_A^{cont})}{(1-\rho^2)\sigma_A} - \frac{\rho(\mu_B^{calm} - \mu_B^{cont})}{(1-\rho^2)\sigma_B}\right)\right]d\widehat{W}_{A,t} \\ &\quad + \left[-y_{A,s}s_A s_B\sigma_B + y_{A,\widehat{p}}\widehat{p}(1-\widehat{p})\left(\frac{(\mu_B^{calm} - \mu_B^{cont})}{(1-\rho^2)\sigma_B} - \frac{\rho(\mu_A^{calm} - \mu_A^{cont})}{(1-\rho^2)\sigma_A}\right)\right]d\widehat{W}_{B,t} \\ &\quad + (y_A(s_A^{A+},\widehat{p}^{A+}) - y_A(s_A,\widehat{p}))d\widehat{N}_A + (y_A(s_A^{B+},\widehat{p}^{B+}) - y_A(s_A,\widehat{p}))d\widehat{N}_B, \end{aligned}$$

where, again, the subscripts s, $\widehat{p}$, ss, $\widehat{p}\widehat{p}$ and $s\widehat{p}$ denote the first and second derivatives with respect to s_A

and $\widehat{p}$. Plugging everything into equation $(A.18)$ leads to the following PDE for y_A:

$$
\begin{aligned}
0 = &\frac{\partial y_A}{\partial t} + \mu_\xi + \phi\widehat{\mu}_A + \frac{1}{2}\phi(\phi-1)\sigma_A^2 + y_{A,s}\mu_s + \frac{1}{2}\left(y_{A,ss} + y_{A,s}^2\right)\sigma_{ss} \\
&+ y_{A,\widehat{p}}\mu_{\widehat{p}} + \frac{1}{2}\left(y_{A,\widehat{p}\widehat{p}} + y_{A,\widehat{p}}^2\right)\sigma_{\widehat{p}\widehat{p}} + y_{A,s}s_A s_B\phi\sigma_A^2 - y_{A,s}s_A s_B\phi\rho\sigma_A\sigma_B \\
&+ \left(y_{A,s\widehat{p}} + y_{A,s}y_{A,\widehat{p}}\right)\sigma_{s\widehat{p}} + y_{A,\widehat{p}}\widehat{p}(1-\widehat{p})(\mu_A^{calm} - \mu_A^{cont})\phi \\
&- \eta_A^{diff}\left(\phi\sigma_A + y_{A,s}s_A s_B\sigma_A - y_{A,s}s_A s_B\rho\sigma_B + y_{A,\widehat{p}}\widehat{p}(1-\widehat{p})\frac{(\mu_A^{calm} - \mu_A^{cont})}{\sigma_A}\right) \\
&- \eta_B^{diff}\left(\phi\rho\sigma_A - y_{A,s}s_A s_B\sigma_B + y_{A,s}s_A s_B\rho\sigma_A + y_{A,\widehat{p}}\widehat{p}(1-\widehat{p})\frac{(\mu_B^{calm} - \mu_B^{cont})}{\sigma_B}\right) \\
&+ \widehat{\lambda}_A\left[(1+\eta_A^{jump})(1+L_A)^\phi e^{y_A(s_A^{A+},\widehat{p}^{A+}) - y_A(s_A,\widehat{p})} - 1\right] \\
&+ \widehat{\lambda}_B\left[(1+\eta_B^{jump})e^{y_A(s_A^{B+},\widehat{p}^{B+}) - y_A(s_A,\widehat{p})} - 1\right].
\end{aligned}
\tag{A.19}
$$

In our numerical solution we do not solve for y_A, but for the price-dividend ratio of the dividend strip itself, i.e. $h_{y,A} = e^{y_A}$. The PDE then changes to the following one:

$$
\begin{aligned}
0 = &\frac{\partial h_{y,A}}{\partial t} + h_{y,A}\mu_\xi + h_{y,A}\phi\widehat{\mu}_A + h_{y,A}\frac{1}{2}\phi(\phi-1)\sigma_A^2 + h_{y,A,s}\mu_s + \frac{1}{2}h_{y,A,ss}\sigma_{ss} \\
&+ h_{y,A,\widehat{p}}\mu_{\widehat{p}} + \frac{1}{2}h_{y,A,\widehat{p}\widehat{p}}\sigma_{\widehat{p}\widehat{p}} + h_{y,A,s}s_A s_B\phi\sigma_A^2 - h_{y,A,s}s_A s_B\phi\rho\sigma_A\sigma_B \\
&+ h_{y,A,s\widehat{p}}\sigma_{s\widehat{p}} + h_{y,A,\widehat{p}}\widehat{p}(1-\widehat{p})(\mu_A^{calm} - \mu_A^{cont})\phi \\
&- \eta_A^{diff}\left(h_{y,A}\phi\sigma_A + h_{y,A,s}s_A s_B\sigma_A - h_{y,A,s}s_A s_B\rho\sigma_B + h_{y,A,\widehat{p}}\widehat{p}(1-\widehat{p})\frac{(\mu_A^{calm} - \mu_A^{cont})}{\sigma_A}\right) \\
&- \eta_B^{diff}\left(h_{y,A}\phi\rho\sigma_A - h_{y,A,s}s_A s_B\sigma_B + h_{y,A,s}s_A s_B\rho\sigma_A + h_{y,A,\widehat{p}}\widehat{p}(1-\widehat{p})\frac{(\mu_B^{calm} - \mu_B^{cont})}{\sigma_B}\right) \\
&+ \widehat{\lambda}_A\left[(1+\eta_A^{jump})(1+L_A)^\phi h_{y,A}(s_A^{A+},\widehat{p}^{A+}) - h_{y,A}(s_A,\widehat{p})\right] \\
&+ \widehat{\lambda}_B\left[(1+\eta_B^{jump})h_{y,A}(s_A^{B+},\widehat{p}^{B+}) - h_{y,A}(s_A,\widehat{p})\right].
\end{aligned}
\tag{A.20}
$$

Given $h_{y,A,t}$ (or its logarithm $y_{A,t}$) we can derive the process for the price of the dividend strip $V_A^T(t)$:

$$
dV_A^T(t) = d\left(h_{y,A,t}D_{A,t}\right) = d\left(e^{y_{A,t}}D_{A,t}\right).
$$

Another application of Itôs Lemma (where we suppress time subscripts again) yields the return of the dividend strip:

$$
\begin{aligned}
R_{y,A,t} = &\frac{dV_A^T(t)}{V_A^T(t)} \\
= &\, dy_A^c + \frac{dD_A^c}{D_A} + \frac{1}{2}d[y^c]_t + \frac{d\left\langle y_A^c, D_A^c\right\rangle}{D_A} + \left((1+L_A)^\phi e^{y_A^{A+} - y_A} - 1\right)d\widehat{N}_A + \left(e^{y_A^{B+} - y_A} - 1\right)d\widehat{N}_B \\
= &\left[\frac{\partial y_A}{\partial t} + y_{A,s}\mu_s + y_{A,\widehat{p}}\mu_{\widehat{p}} + \frac{1}{2}\left(y_{A,ss} + y_{A,s}^2\right)\sigma_{ss} + \frac{1}{2}\left(y_{A,\widehat{p}\widehat{p}} + y_{A,\widehat{p}}^2\right)\sigma_{\widehat{p}\widehat{p}} + \left(y_{A,s\widehat{p}} + y_{A,s}y_{A,\widehat{p}}\right)\sigma_{s\widehat{p}}\right. \\
&\left. + \phi\widehat{\mu}_A + \frac{1}{2}\phi(\phi-1)\sigma_A^2 + y_{A,s}s_A s_B\left(\phi\sigma_A^2 - \phi\rho\sigma_A\sigma_B\right) + y_{A,\widehat{p}}\widehat{p}(1-\widehat{p})\left(\mu_A^{calm} - \mu_A^{cont}\right)\phi\right]dt
\end{aligned}
$$

$$
\begin{aligned}
&+\left[\phi\sigma_A + y_{A,s}s_A s_B\sigma_A + y_{A,\widehat{p}}\widehat{p}(1-\widehat{p})\left(\frac{(\mu_A^{calm}-\mu_A^{cont})}{(1-\rho^2)\sigma_A} - \frac{(\mu_B^{calm}-\mu_B^{cont})\rho}{(1-\rho^2)\sigma_B}\right)\right] d\widehat{W}_A \\
&+\left[-y_{A,s}s_A s_B\sigma_B + y_{A,\widehat{p}}\widehat{p}(1-\widehat{p})\left(\frac{(\mu_B^{calm}-\mu_B^{cont})}{(1-\rho^2)\sigma_B} - \frac{(\mu_A^{calm}-\mu_A^{cont})\rho}{(1-\rho^2)\sigma_A}\right)\right] d\widehat{W}_B \\
&+\left((1+L_A)^{\phi}e^{y_A(s^{A+},\widehat{p}^{A+})-y_A(s,\widehat{p})}-1\right)d\widehat{N}_A + \left(e^{y_A(s^{B+},\widehat{p}^{B+})-y_A(s,\widehat{p})}-1\right)d\widehat{N}_B.
\end{aligned}
$$

Note that the dividend strip is a claim on the time T dividend of asset A. There are thus no intermediate dividends and thus no dividend yield appearing in the definition of the return. The expected return of the dividend strip is given by

$$
\begin{aligned}
\frac{E_t[R_{y,A,t}]}{dt} &= \frac{E_t[dV_A^T(t)]}{V_A^T(t)} \\
&= \frac{\partial y_A}{\partial t} + y_{A,s}\mu_s + y_{A,\widehat{p}}\mu_{\widehat{p}} + \frac{1}{2}\left(y_{A,ss}+y_{A,s}^2\right)\sigma_{ss} + \frac{1}{2}\left(y_{A,\widehat{p}\widehat{p}}+y_{A,\widehat{p}}^2\right)\sigma_{\widehat{p}\widehat{p}} + \left(y_{A,s\widehat{p}}+y_{A,s}y_{A,\widehat{p}}\right)\sigma_{s\widehat{p}} \\
&\quad + \phi\widehat{\mu}_A + \frac{1}{2}\phi(\phi-1)\sigma_A^2 + y_{A,s}s_A s_B\left(\phi\sigma_A^2 - \phi\rho\sigma_A\sigma_B\right) + y_{A,\widehat{p}}\widehat{p}(1-\widehat{p})\left(\mu_A^{calm}-\mu_A^{cont}\right)\phi \\
&\quad + \widehat{\lambda}_A\left((1+L_A)^{\phi}e^{y_A(s^{A+},\widehat{p}^{A+})-y_A(s,\widehat{p})}-1\right) + \widehat{\lambda}_B\left(e^{y_A(s^{B+},\widehat{p}^{B+})-y_A(s,\widehat{p})}-1\right).
\end{aligned}
$$

Finally, the local variance of the return of the dividend strip satisfies

$$
\begin{aligned}
\frac{d\left\langle V_A^T(t)\right\rangle}{(V_A^T(t))^2 dt} &= \left(\phi\sigma_A + y_{A,s}s_A s_B\sigma_A + y_{A,\widehat{p}}\widehat{p}(1-\widehat{p})\left(\frac{(\mu_A^{calm}-\mu_A^{cont})}{(1-\rho^2)\sigma_A} - \frac{(\mu_B^{calm}-\mu_B^{cont})\rho}{(1-\rho^2)\sigma_B}\right)\right)^2 \\
&\quad + \left(-y_{A,s}s_A s_B\sigma_B + y_{A,\widehat{p}}\widehat{p}(1-\widehat{p})\left(\frac{(\mu_B^{calm}-\mu_B^{cont})}{(1-\rho^2)\sigma_B} - \frac{(\mu_A^{calm}-\mu_A^{cont})\rho}{(1-\rho^2)\sigma_A}\right)\right)^2 \\
&\quad + 2\rho\left(\phi\sigma_A + y_{A,s}s_A s_B\sigma_A + y_{A,\widehat{p}}\widehat{p}(1-\widehat{p})\left(\frac{(\mu_A^{calm}-\mu_A^{cont})}{(1-\rho^2)\sigma_A} - \frac{(\mu_B^{calm}-\mu_B^{cont})\rho}{(1-\rho^2)\sigma_B}\right)\right) \\
&\qquad \cdot\left(-y_{A,s}s_A s_B\sigma_B + y_{A,\widehat{p}}\widehat{p}(1-\widehat{p})\left(\frac{(\mu_B^{calm}-\mu_B^{cont})}{(1-\rho^2)\sigma_B} - \frac{(\mu_A^{calm}-\mu_A^{cont})\rho}{(1-\rho^2)\sigma_A}\right)\right) \\
&\quad + \widehat{\lambda}_A\left((1+L_A)^{\phi}e^{y_A(s^{A+},\widehat{p}^{A+})-y_A(s,\widehat{p})}-1\right)^2 + \widehat{\lambda}_B\left(e^{y_A(s^{B+},\widehat{p}^{B+})-y_A(s,\widehat{p})}-1\right)^2.
\end{aligned}
$$

B Properties of Price-to-fundamentals Ratios

To foster some intuition of the properties of the price-to-fundamentals ratio derived above, we look at the solution of those PDEs when using the benchmark calibration as reported in the first column of Table 1 in the following.

The upper left graph in Figure 2 depicts the wealth-consumption ratio as a function of the state variables s_A and $\widehat{p}$. First of all, it is concave in s_A and the largest for $s_A = 0.5$. As the dynamics in (7) show, aggregate consumption is the least risky for intermediate values of s_A, implying that the wealth-consumption ratio is the largest in this case. More importantly, the wealth-consumption ratio is monotonically decreasing in $\widehat{p}$. On the one hand, a lower probability $\widehat{p}$ implies a smaller perceived expected growth rate of consumption and a higher perceived intensity for consumption shocks. In an economy with recursive utility and a preference for early resolution of uncertainty, both lower expected

growth rates and higher risk decrease asset prices, and this effect is present in our model as well. On the other hand, the uncertainty in the economy is the highest for intermediate values of $\widehat{p}$ as can be seen from equation (5). Both the diffusive volatility and the jump size of $\widehat{p}$ are the largest for $\widehat{p}$ around 0.5. This additional uncertainty drives down the wealth-consumption ratio. Altogether, the figure however shows that the first effect is dominating and the wealth-consumption ratio is almost linearly decreasing in $\widehat{p}$.

The lower panel of Figure 2 depicts the price-dividend ratios of the two assets in the $[s_A, \widehat{p}]$-space for the benchmark case. First of all, as already discussed by Cochrane, Longstaff, and Santa-Clara (2008) and Martin (2013), the price-dividend ratios are monotonic functions of the output share of the respective tree. In an equilibrium with two Lucas trees, small assets are more valuable from a diversification perspective. Ideally, the investor would like to hold a diversified portfolio with equal shares of both trees. Since markets have to clear in equilibrium, the price of the tree with the smaller output has to go up relative to its cash flow. Looking at dividends (as levered output) instead of output itself leaves this argument qualitatively unchanged. Finally, similar to the wealth-consumption ratio, the price-dividend ratios are monotonic and convex in $\widehat{p}$. Note however that the impact of $\widehat{p}$ is much smaller than the diversification effect through s_A. Along the s_A dimension the changes in the price-dividend ratio range from 69% to 72% whereas along the $\widehat{p}$ dimension, the difference is only between 9.3% and 12.7%.

References

Ait-Sahalia, Y., J. Cacho-Diaz, and R. Laeven (2013): "Modeling Financial Contagion Using Mutually Exciting Jump Processes," *Working Paper*.

Backus, D., M. Chernov, and I. Martin (2011): "Disasters Implied by Equity Index Options," *Journal of Finance*, 66(6), 1969–2012.

Bansal, R., D. Kiku, I. Shaliastovich, and A. Yaron (2013): "Volatility, the Macroeconomy, and Asset Prices," *forthcoming: Journal of Finance*.

Bansal, R., and A. Yaron (2004): "Risks for the Long Run: A Potential Resolution of Asset Pricing Puzzles," *The Journal of Finance*, 59, 1481–1509.

Barro, R. (2006): "Rare Disasters and Asset Markets in the Twentieth Century," *Quarterly Journal of Economics*, 121(3), 823–866.

Barro, R. J. (2009): "Rare Disasters, Asset Prices, and Welfare Costs," *American Economic Review*, 99(1), 243–264.

Belo, F., P. Collin-Dufresne, and R. S. Goldstein (2012): "Endogenous Dividend Dynamics and the Term Structure of Dividend Strips," *Working Paper*.

Benzoni, L., P. Collin-Dufresne, R. Goldstein, and J. Helwege (2011): "Modeling Credit Contagion Via the Updating of Fragile Beliefs: An Investigation of the European Sovereign Crisis," *Working Paper*.

Benzoni, L., P. Collin-Dufresne, and R. S. Goldstein (2011): "Explaining asset pricing puzzles associated with the 1987 market crash," *Journal of Financial Economics*, 101(3), 552–573.

Boguth, O., M. Carlson, A. Fisher, and M. Simutin (2012): "Leverage and the Limits of Arbitrage Pricing: Implications for Dividend Strips and the Term Structure of Equity Risk Premia," *Working Paper*.

Branger, N., H. Kraft, and C. Meinerding (2013a): "How Does Contagion Affect General Equilibrium Asset Prices?," *Working Paper*.

——— (2013b): "Partial Information about Contagion Risk, Self-Exciting Processes and Portfolio Optimization," *forthcoming: Journal of Economic Dynamics and Control*.

Brennan, M., and Y. Xia (2001): "Stock Return Volatility and Equity Premium," *Journal of Monetary Economics*, 47(2), 249–283.

Buraschi, A., and P. Porchia (2012): "Dynamic Networks and Asset Pricing," *Working Paper*.

Campbell, J., G. Chacko, J. Rodriguez, and L. Viceira (2004): "Strategic Asset Allocation in a Continuous-Time VAR Model," *Journal of Economic Dynamics and Control*, 28(11), 2195–2214.

Chen, H., S. Joslin, and N.-K. Tran (2012): "Rare Disasters and Risk Sharing," *Review of Financial Studies*, 25(7), 2189–2224.

Cochrane, J. (2008): "The Dog That Did Not Bark: A Defense of Return Predictability," *Review of Financial Studies*, 21(4), 1533–1575.

Cochrane, J., F. Longstaff, and P. Santa-Clara (2008): "Two Trees," *Review of Financial Studies*, 21(1), 347–385.

Collin-Dufresne, P., M. Johannes, and L. A. Lochstoer (2013): "Parameter Learning in General Equilibrium: The Asset Pricing Implications," *Working Paper*.

Constantinides, G. (2008): "Comment on 'Macroeconomic Crises since 1870' by Barro and Ursua," *Brookings Papers on Economic Activity*, pp. 341–350.

Croce, M., M. Lettau, and S. Ludvigson (2012): "Investor Information, Long-Run Risk and the Term Structure of Equity," *Working Paper*.

Duffie, D., and L. G. Epstein (1992a): "Asset Pricing with Stochastic Differential Utility," *Review of Financial Studies*, 5(3), 411–436.

——— (1992b): "Stochastic Differential Utility," *Econometrica*, 60(2), 353–394.

Ehling, P., and C. Heyerdahl-Larsen (2013): "Correlations," *Working Paper*.

Epstein, L., and S. Zin (1989): "Substitution, Risk Aversion, and the Temporal Behavior of Consumption Growth and Asset Returns I: A Theoretical Framework," *Econometrica*, 57(4), 937–969.

Frey, R., and W. Runggaldier (2010): "Pricing Credit Derivatives under Incomplete Information: A Nonlinear-Filtering Approach," *Finance and Stochastics*, 16(1), 105–133.

Lauricella, T. (2009): "Failure of a Fail-Safe Strategy Sends Investors Scrambling," *Wall Street Journal*, July 10.

Lettau, M., and J. Wachter (2007): "Why is Long-Horizon Equity Less Risky? A Duration-Based Explanation of the Value Premium," *Journal of Finance*, 62(1), 55–92.

Longin, F., and B. Solnik (2001): "Extreme Correlation of International Equity Markets," *The Journal of Finance*, LVI(2), 649–676.

Lustig, H., S. van Nieuwerburgh, and A. Verdelhan (2013): "The Wealth-Consumption Ratio," *The Review of Asset Pricing Studies*, 3(1), 38–94.

Ma, T., and Q. Yu (1989): "The Keldys-Fichera Boundary Value Problems for Degenerate Quasielliptic Equations of Second Order," *Differential and Integral Equations*, 2(4), 379–388.

Martin, I. (2013): "The Lucas Orchard," *Econometrica*, 81(1), 55–111.

Mele, A. (2007): "Asymmetric stock market volatility and the cyclical behavior of expected returns," *Journal of Financial Economics*, 86, 446–478.

Menzly, L., T. Santos, and P. Veronesi (2004): "Understanding Predictability," *Journal of Political Economy*, 112(1), 1–47.

Nakamura, E., J. Steinsson, R. J. Barro, and J. Ursúa (2013): "Crises and Recoveries in an Empirical Model of Consumption Disasters," *American Economic Journal: Macroeconomics*, 5(3), 35–74.

Oleinik, O., and E. Radkevich (1973): *Second Order Equations with Nonnegative Characteristic Form*. Plenum Press, New York.

Pakos, M. (2012): "Consumption, Asset Prices and Persistent Economic Uncertainty," *Working Paper*.

Pástor, L., and P. Veronesi (2009): "Learning in Financial Markets," *Annual Review of Financial Economics*, 1, 361–381.

van Binsbergen, J., M. Brandt, and R. Koijen (2012): "On the Timing and Pricing of Dividends," *American Economic Review*, 102(4), 1596–1618.

Veronesi, P. (1999): "Stock Market Overreaction to Bad News in Good Times: A Rational Expectations Equilibrium Model," *Review of Financial Studies*, 12(5), 975–1007.

Wachter, J. (2013): "Can time-varying risk of rare disasters explain aggregate stock market volatility?," *Journal of Finance*, 68(3), 987–1035.

	Benchmark Identical Trees	Toxic vs. Non-Toxic Assets	Robust vs. Contagion-Sensitive Assets	Large vs. Small Growth Spread
μ_A^{calm}	0.047	0.047	0.047	0.055
μ_A^{cont}	0.019	0.019	0.019	0.011
μ_B^{calm}	0.047	0.047	0.047	0.039
μ_B^{cont}	0.019	0.019	0.019	0.027
σ_A	0.01	0.01	0.01	0.01
σ_B	0.01	0.01	0.01	0.01
ρ	0	0	0	0
L_A	-0.06	-0.06	-0.06	-0.06
L_B	-0.06	-0.06	-0.06	-0.06
$\lambda_A^{calm,calm}$	0.125	0.00	0.125	0.125
$\lambda_A^{calm,cont}$	0.125	0.25	0.125	0.125
$\lambda_B^{calm,calm}$	0.125	0.25	0.125	0.125
$\lambda_B^{calm,cont}$	0.125	0.00	0.125	0.125
$\lambda_A^{cont,cont}$	0.80	0.80	0.65	0.80
$\lambda_B^{cont,cont}$	0.80	0.80	0.95	0.80
$\lambda^{cont,calm}$	1	1	1	1
ϕ	2.5	2.5	2.5	2.5
β	0.039	0.039	0.039	0.039
γ	10	10	10	10
ψ	2	2	2	2

Table 1: Parameters

The table reports the parameters of the output processes and of the investor's utility function. The first column refers to the benchmark calibration discussed in Sections 3 and 4. The other three columns give the parameters for the three cases discussed in Section 4.9.

	Benchmark Calibration with $s_{A,0} = 0.5$			**Data**			**Benchmark Calibration with $s_{A,0} = 0.67$**			**Benchmark Calibration with $s_{A,0} = 0.75$**			**Benchmark Calibration with $s_{A,0} = 0.83$**		
Quantity	$E[\cdot]$	$\sigma(\cdot)$	$AC1(\cdot)$	$E[\cdot]$	$\sigma(\cdot)$	$AC1(\cdot)$	$E[\cdot]$	$\sigma(\cdot)$	$AC1(\cdot)$	$E[\cdot]$	$\sigma(\cdot)$	$AC1(\cdot)$	$E[\cdot]$	$\sigma(\cdot)$	$AC1(\cdot)$
Δc	0.019	0.028	0.21	0.019	0.013	0.42	0.019	0.028	0.21	0.019	0.028	0.21	0.019	0.028	0.21
Δd	0.048	0.074	0.20	0.022	0.066	0.25	0.048	0.074	0.20	0.048	0.074	0.20	0.048	0.074	0.19
Δd_A	0.048	0.098	0.13	0.024	0.133	-	0.048	0.098	0.13	0.048	0.098	0.13	0.048	0.098	0.13
Δd_B	0.048	0.098	0.13	0.024	0.133	-	0.048	0.098	0.13	0.048	0.098	0.13	0.048	0.098	0.13
$w - c$	3.33	0.010	0.48	4.63	0.247	0.86	3.32	0.011	0.52	3.31	0.011	0.55	3.30	0.011	0.57
$p - d$	3.09	0.046	0.59	3.38	0.423	0.88	3.12	0.050	0.66	3.15	0.054	0.72	3.21	0.062	0.79
$p_A - d_A$	3.12	0.056	0.74	-	-	-	2.98	0.053	0.67	2.91	0.051	0.64	2.85	0.050	0.59
$p_B - d_B$	3.12	0.056	0.74	-	-	-	3.28	0.060	0.78	3.39	0.061	0.80	3.52	0.061	0.82
$corr(r_A, r_B)$	0.59	0.385	-	0.72	-	-	0.59	0.386	-	0.59	0.387	-	0.58	0.390	-
$\widehat{p}$	0.80	0.304	0.46	0.80	-	-	0.80	0.306	0.46	0.80	0.306	0.46	0.80	0.306	0.46
r_f	0.035	0.013	0.46	0.013	0.027	-	0.034	0.013	0.46	0.033	0.013	0.46	0.032	0.014	0.46
r_{Aggr}	0.092	0.111	0.01	0.082	0.181	-	0.094	0.111	0.01	0.091	0.111	0.01	0.090	0.110	0.01
r_A	0.092	0.124	0.01	-	-	-	0.098	0.127	-0.01	0.102	0.128	-0.01	0.106	0.130	-0.01
r_B	0.092	0.124	0.01	-	-	-	0.085	0.121	0.01	0.082	0.120	0.02	0.078	0.119	0.02
$r_{Aggr} - r_f$	0.058	0.111	-0.05	0.069	0.174	-0.01	0.059	0.111	-0.04	0.059	0.110	-0.04	0.058	0.109	-0.04
$r_A - r_f$	0.058	0.123	-0.03	-	-	-	0.064	0.126	-0.04	0.068	0.127	-0.05	0.074	0.129	-0.05
$r_B - r_f$	0.058	0.123	-0.03	-	-	-	0.050	0.121	-0.03	0.048	0.119	-0.02	0.046	0.118	-0.02
$E[r_A - r_f]$	0.058	0.009	0.33	-	-	-	0.064	0.010	0.38	0.068	0.010	0.40	0.074	0.011	0.40
$E[r_B - r_f]$	0.058	0.009	0.33	-	-	-	0.050	0.009	0.32	0.048	0.010	0.34	0.046	0.010	0.36

Table 2: Main Model Results

The Table reports the means, volatilities and annual autocorrelations of the main quantities of the model for the benchmark calibration. The numbers in the first column for an initial output share $s_{A,0} = 0.5$ are analyzed in Section 4. The results with initial output shares $s_{A,0} = 0.67, 0.75$ and 0.83 are discussed in Section 4.9. All results have been obtained via Monte Carlo simulations with simulation horizon 65 years, daily frequency and 10000 sample paths. All moments are annual except for the correlation which is calculated for monthly returns. The volatilities of $corrr_A, r_B$ and $\widehat{p}$ are calculated using non-overlapping 4-year windows. The column labeled 'Data' reports mostly numbers from Benzoni, Collin-Dufresne, and Goldstein (2011) who use data from 1946 to 2008. The statistics on the risk-free rate refer to the 3-month T-bill rate as reported by Wachter (2013). The statistics on correlations and sectoral dividends are from Ehling and Heyerdahl-Larsen (2013) and, finally, details about the wealth-consumption ratio and several autocorrelations have been reported by either Lustig, van Nieuwerburgh, and Verdelhan (2013) or Bansal, Kiku, Shaliastovich, and Yaron (2013).

	Horizon (in years)			
	1	2	3	4
	Panel A: Our Model			
β	-0.14	-0.15	-0.16	-0.16
R^2	0.24	0.30	0.33	0.34
$E[\widehat{p}]$	0.80	0.80	0.80	0.80
$\sigma(\widehat{p})$	0.31	0.27	0.24	0.21
$E[\sigma(r_A)]$	0.09	0.10	0.11	0.11
$\sigma(\sigma(r_A))$	0.09	0.07	0.06	0.05

Table 3: Regressions of Monthly Return Volatilities

The table reports summary statistics and regression coefficients for the regressions of return volatilities of asset A on the state of the economy as discussed in Section 4.5. The beta coefficients and summary statistics for the return volatilities are annualized. The volatilities of returns have been computed from simulated monthly returns using a 1-/2-/3- or 4-year rolling window. The independent variable is the integral of the state variable $\widehat{p}$ over that same period. All results have been obtained using the parameters from the benchmark calibration in the first column of Table 1.

	Horizon (in years)			
	1	2	3	4
	Panel A: Our Model			
β	-0.38	-0.30	-0.23	-0.18
R^2	0.09	0.07	0.06	0.06
$E[\widehat{p}]$	0.80	0.80	0.80	0.80
$\sigma(\widehat{p})$	0.31	0.27	0.24	0.21
$E[corr(r_A, r_B)]$	0.47	0.54	0.58	0.60
$\sigma(corr(r_A, r_B))$	0.39	0.31	0.28	0.22

Table 4: Regressions of Monthly Return Correlations

The table reports summary statistics and regression coefficients for the regressions of correlations on the state of the economy as discussed in Section 4.6. The correlations have been computed from simulated monthly returns using a 1-/2-/3- or 4-year rolling window. The independent variable is the integral of the state variable $\widehat{p}$ over that same period. All results have been obtained using the parameters from the benchmark calibration in the first column of Table 1.

	Horizon (in years)					
	1	2	4	6	8	10
	Panel A: Our Model					
β	-0.19	-0.28	-0.38	-0.47	-0.56	-0.64
R^2	0.03	0.03	0.04	0.05	0.05	0.06
	Panel B: Wachter (2013)					
β	-0.11	-0.22	-0.40	-0.56	-0.69	-0.82
R^2	0.04	0.08	0.15	0.20	0.23	0.26
	Panel C: Data					
β	-0.13	-0.23	-0.33	-0.48	-0.64	-0.86
R^2	0.09	0.17	0.23	0.30	0.38	0.43

Table 5: Long Horizon Predictive Regressions: Excess Returns

Panel A of the table reports the results from long-horizon predictive regressions $\sum_{\tau=t}^{t+h-1} r_{aggr,\tau,\tau+1} - r_{f,\tau,\tau+1} = \alpha + \beta\ w_{aggr,t} + \varepsilon_t$ with simulated model data. More specifically, $r_{aggr,\tau,\tau+1}$ denotes the log return on the aggregate dividend claim from year τ to year $\tau+1$, $r_{f,\tau,\tau+1}$ denotes the return on a risk-free bond from time τ to time $\tau+1$ and $w_{aggr,t}$ is the log price-dividend ratio of the aggregate dividend claim at time t. We proxy $r_{f,\tau,\tau+1}$ by integrating the monthly simulated risk-free short rates. The table reports results for different horizons of $h = 1, 2, 4, 6, 8, 10$ years. All results have been obtained using the benchmark calibration from the first column of Table 1. Panel B and C are taken from Wachter (2013).

	Horizon (in years)					
	1	2	4	6	8	10
	Panel A: Our Model					
β	0.02	0.03	0.02	0.02	0.02	0.02
R^2	0.11	0.08	0.05	0.04	0.04	0.04
	Panel B: Wachter (2013)					
β	0.02	0.04	0.07	0.10	0.12	0.13
R^2	0.01	0.02	0.04	0.05	0.06	0.06
	Panel C: Data					
β	-0.001	-0.006	-0.009	-0.011	-0.016	-0.014
R^2	0.0006	0.0137	0.0164	0.0180	0.0268	0.0162

Table 6: Long Horizon Predictive Regressions: Consumption Growth

Panel A of the table reports the results from long-horizon predictive regressions as in Table 5, but growth rates of aggregate consumption as dependent variable. Again, all results have been obtained using the benchmark calibration from the first column of Table 1. Panel B and C are again taken from Wachter (2013).

	Benchmark Calibration			**Data**			**Toxic vs. Non-Toxic Assets**			**Robust vs. Contagion-Sensitive Assets**			**Large vs. Small Growth Spread**		
Quantity	$E[\cdot]$	$\sigma(\cdot)$	$AC1(\cdot)$	$E[\cdot]$	$\sigma(\cdot)$	$AC1(\cdot)$	$E[\cdot]$	$\sigma(\cdot)$	$AC1(\cdot)$	$E[\cdot]$	$\sigma(\cdot)$	$AC1(\cdot)$	$E[\cdot]$	$\sigma(\cdot)$	$AC1(\cdot)$
Δc	0.019	0.028	0.21	0.019	0.013	0.42	0.019	0.028	0.21	0.019	0.028	0.21	0.020	0.029	0.21
Δd	0.048	0.073	0.20	0.022	0.066	0.25	0.048	0.074	0.20	0.050	0.073	0.19	0.054	0.079	0.20
Δd_A	0.048	0.098	0.13	0.024	0.133	-	0.048	0.098	0.17	0.053	0.094	0.11	0.060	0.099	0.17
Δd_B	0.048	0.098	0.13	0.024	0.133	-	0.048	0.098	0.09	0.043	0.103	0.15	0.036	0.098	0.09
$w - c$	3.33	0.010	0.48	4.63	0.247	0.86	3.33	0.011	0.51	3.34	0.010	0.53	3.32	0.011	0.54
$p - d$	3.09	0.046	0.59	3.43	0.423	0.88	3.11	0.050	0.65	3.34	0.063	0.85	3.06	0.065	0.77
$p_A - d_A$	3.12	0.056	0.74	-	-	-	3.03	0.053	0.79	3.29	0.051	0.77	3.07	0.083	0.81
$p_B - d_B$	3.12	0.056	0.74	-	-	-	3.23	0.059	0.67	3.57	0.232	0.97	3.14	0.060	0.89
$corr(r_A, r_B)$	0.59	0.385	-	0.72	-	-	0.61	0.378	-	0.81	0.216	-	0.57	0.380	-
$\widehat{p}$	0.80	0.304	0.46	0.80	-	-	0.80	0.309	0.46	0.80	0.306	0.46	0.80	0.308	0.46
r_f	0.035	0.013	0.46	0.013	0.027	-	0.034	0.012	0.46	0.085	0.012	0.46	0.034	0.013	0.46
r_{Aggr}	0.092	0.111	0.01	0.082	0.181	-	0.094	0.111	0.00	0.055	0.103	0.03	0.100	0.118	0.01
r_A	0.092	0.124	0.01	-	-	-	0.096	0.130	0.02	0.089	0.115	0.01	0.104	0.136	0.00
r_B	0.092	0.124	0.01	-	-	-	0.088	0.116	−0.01	0.078	0.099	0.07	0.082	0.111	0.01
$r_{Aggr} - r_f$	0.058	0.111	-0.05	0.069	0.174	-0.01	0.059	0.110	-0.04	0.050	0.103	-0.01	0.065	0.117	-0.05
$r_A - r_f$	0.058	0.123	-0.03	-	-	-	0.061	0.129	-0.02	0.054	0.114	-0.03	0.070	0.135	-0.04
$r_B - r_f$	0.058	0.123	-0.03	-	-	-	0.053	0.115	-0.04	0.043	0.099	0.02	0.046	0.111	-0.02
$E[r_A - r_f]$	0.058	0.009	0.33	0.069	-	-	0.061	0.010	0.48	0.054	0.008	0.36	0.070	0.013	0.58
$E[r_B - r_f]$	0.058	0.009	0.33	0.069	-	-	0.053	0.007	0.31	0.043	0.008	0.57	0.046	0.007	0.46

Table 7: Model Results for Different Calibrations

The Table reports the means, volatilities and annual autocorrelations of the main quantities of the model for all parameter calibrations from Table 1. The results have been obtained via Monte Carlo simulations as in Table 2, but with initial value $s_{A,0} = 0.5$. The column labeled 'Data' is the same as in Table 2.

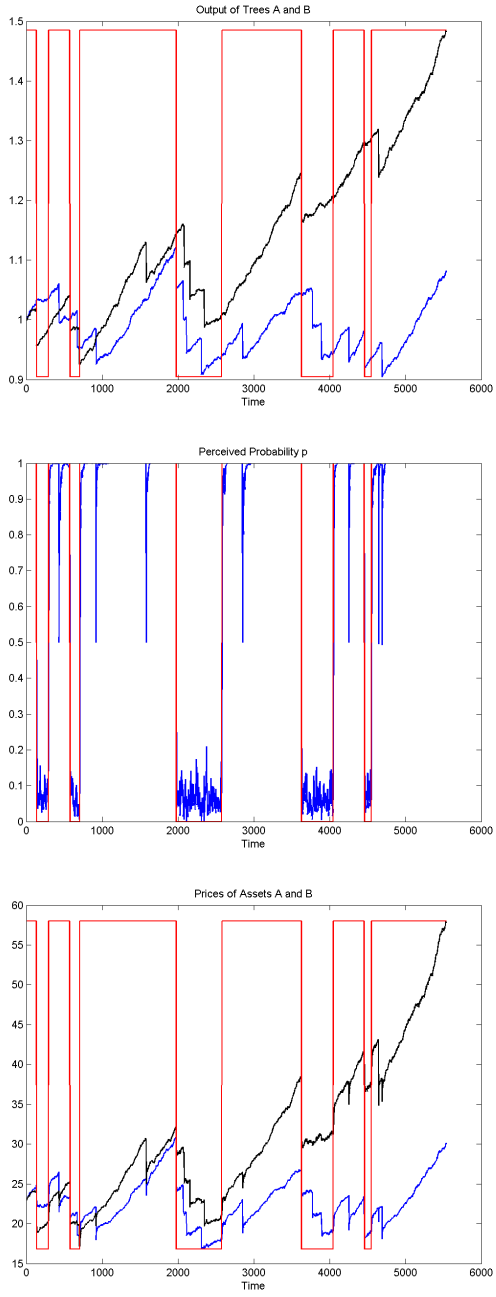

Figure 1: Sample Paths of our Economy

From top to bottom the graphs in the figure depict exemplary random paths for the output of the two trees (black and blue line) together with the true state (red line), the resulting path of the estimated probability $\widehat{p}$ (blue) together with true state (red), and the resulting paths of the prices of the two assets (black and blue) together with true state (red). The results have been obtained using the benchmark calibration shown in the first column of Table 1.

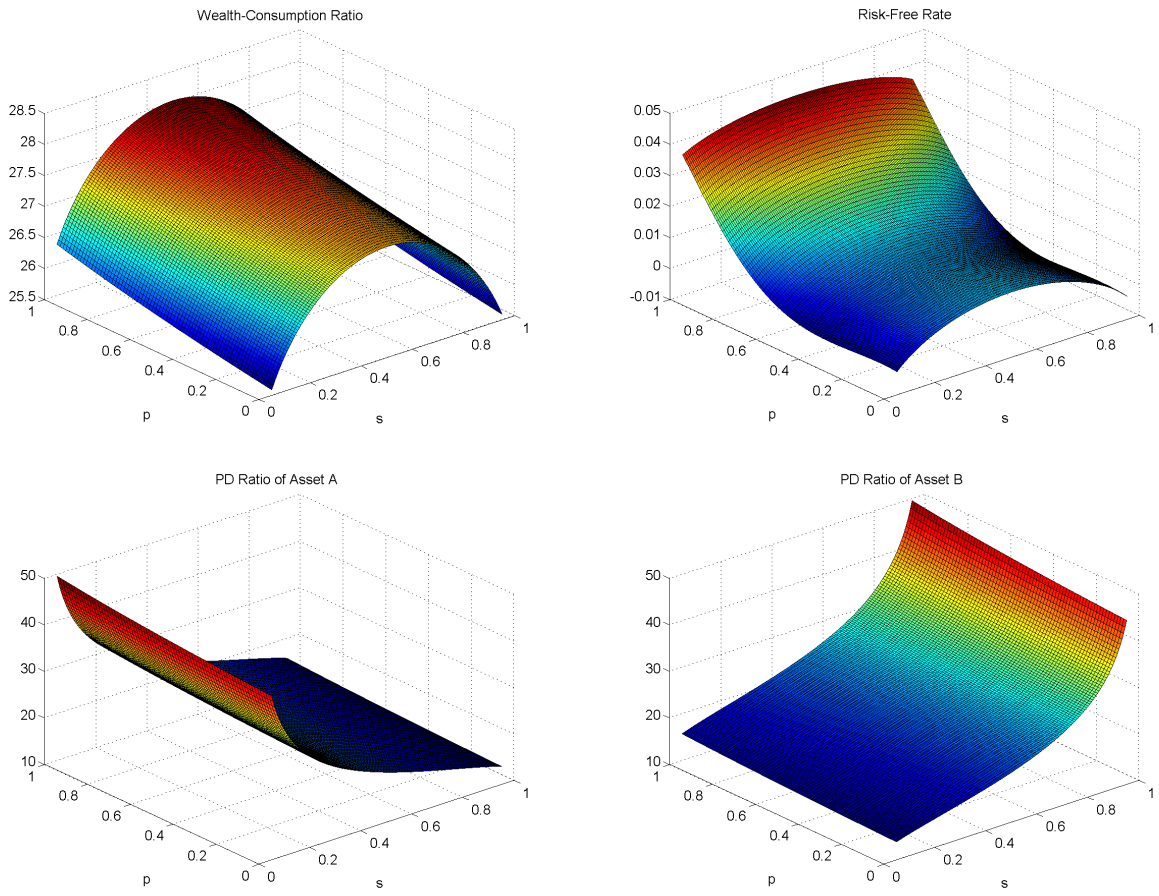

Figure 2: Wealth-Consumption Ratio, Risk-free Rate, PD Ratios of Assets A and B

The figure depicts the wealth-consumption ratio (upper left picture), the risk-free rate (upper right picture) and the price-dividend ratios of asset A (lower left picture) and asset B (lower right picture) as functions of the two state variables s_A and $\widehat{p}$. The results have been obtained using the benchmark calibration shown in the first column of Table 1.

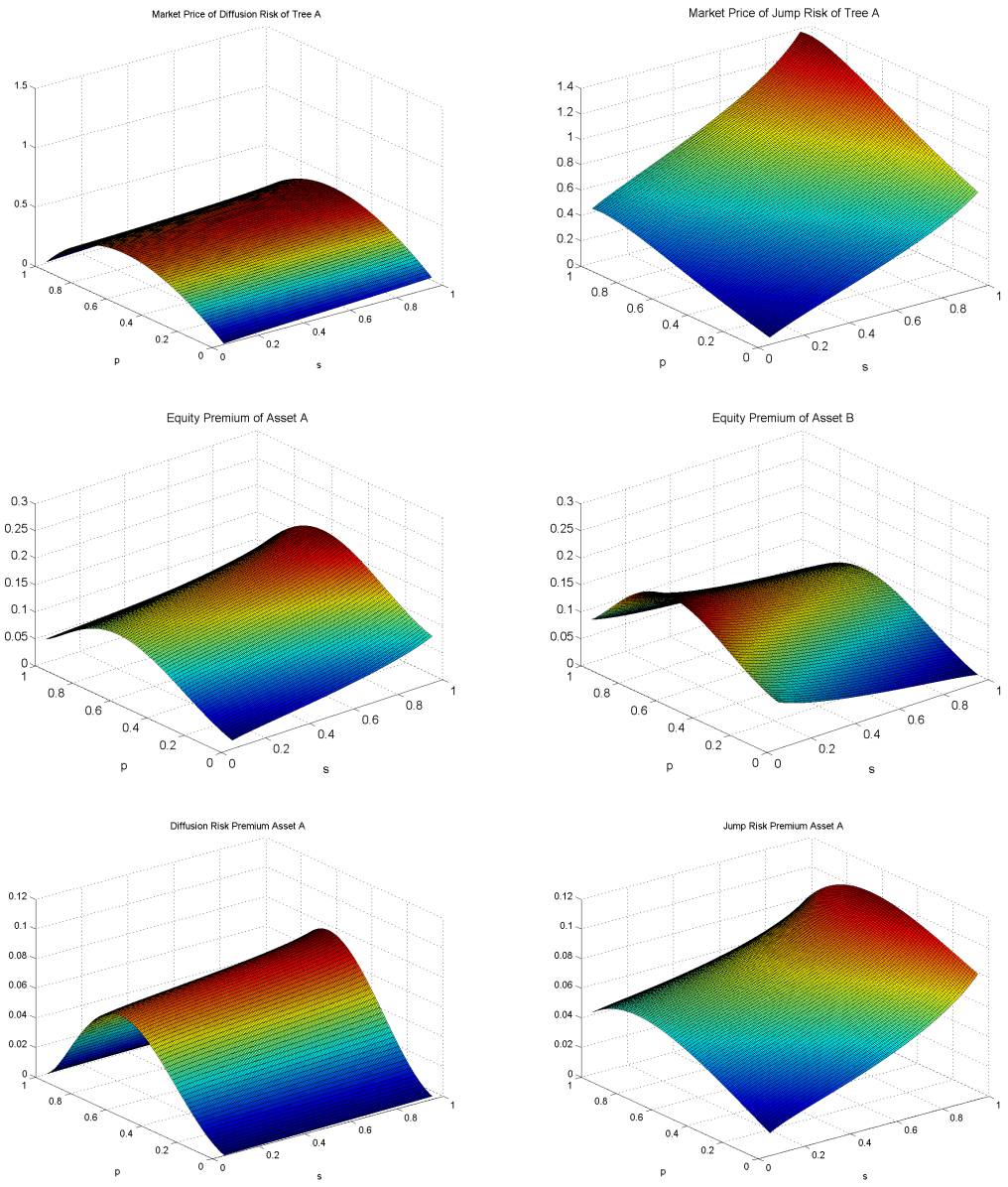

Figure 3: Market Prices of Risk, Equity Premia of Assets A and B, Decomposition of Equity Premium of Asset A

The figure depicts the market price of diffusion risk of tree A (upper left picture) and the market price of jump risk of tree A (upper right picture), the equity premia of asset A (middle left picture) and asset B (middle right picture) and the decomposition of the equity premium of asset A into a diffusion risk premium (lower left picture) and a jump risk premium (lower right picture) as functions of the two state variables s_A and $\widehat{p}$. The decomposition of the equity premium is discussed in Section 4.4. The results have been obtained using the benchmark calibration shown in the first column of Table 1.

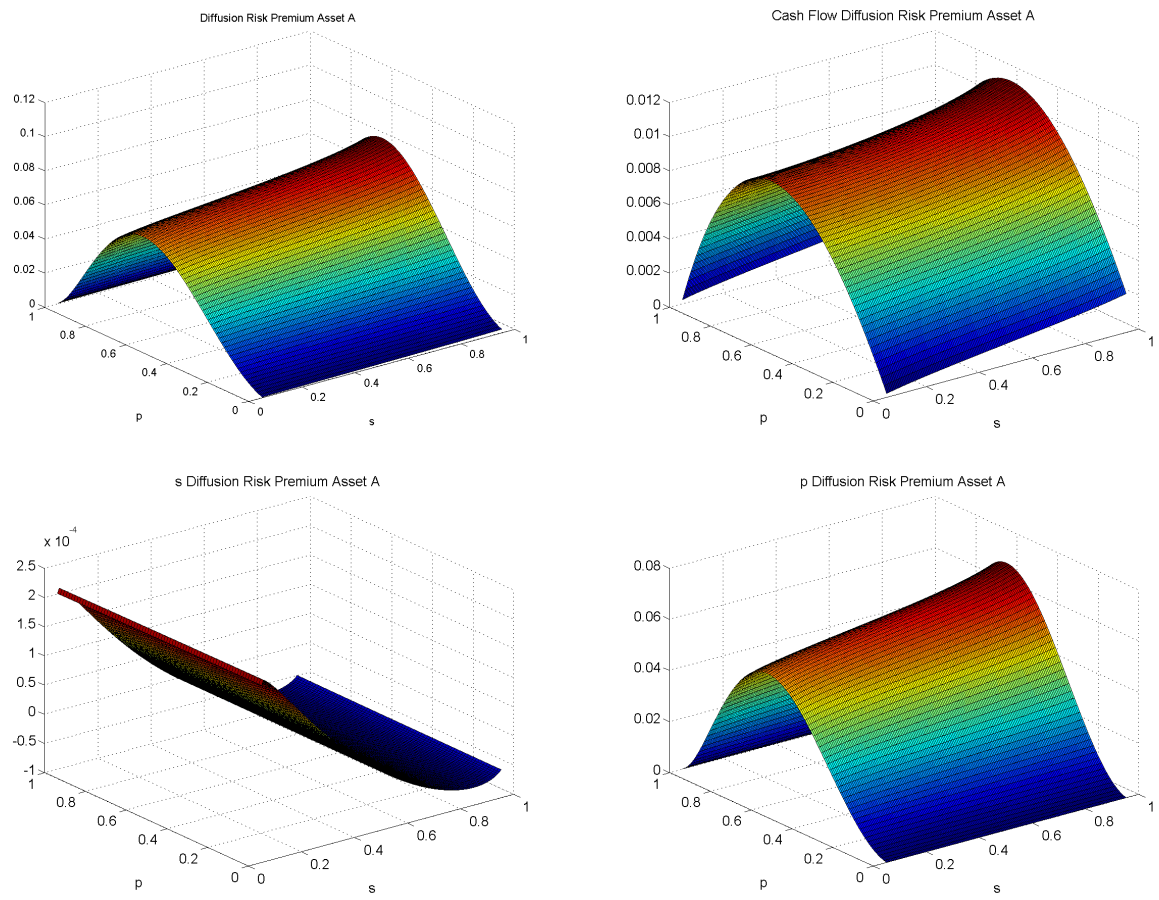

Figure 4: Diffusion Premia for Asset A

The figure depicts a decomposition of the diffusion risk premium of asset A (upper left picture), which is also shown in Figure 3, into three components: a cash flow risk premium (upper right picture), a premium for diffusive s_A-risk (lower left picture) and a premium for diffusive $\widehat{p}$-risk (lower right picture). The independent variables in all graphs are the two state variables s_A and $\widehat{p}$. The results have been obtained using the benchmark calibration shown in the first column of Table 1.

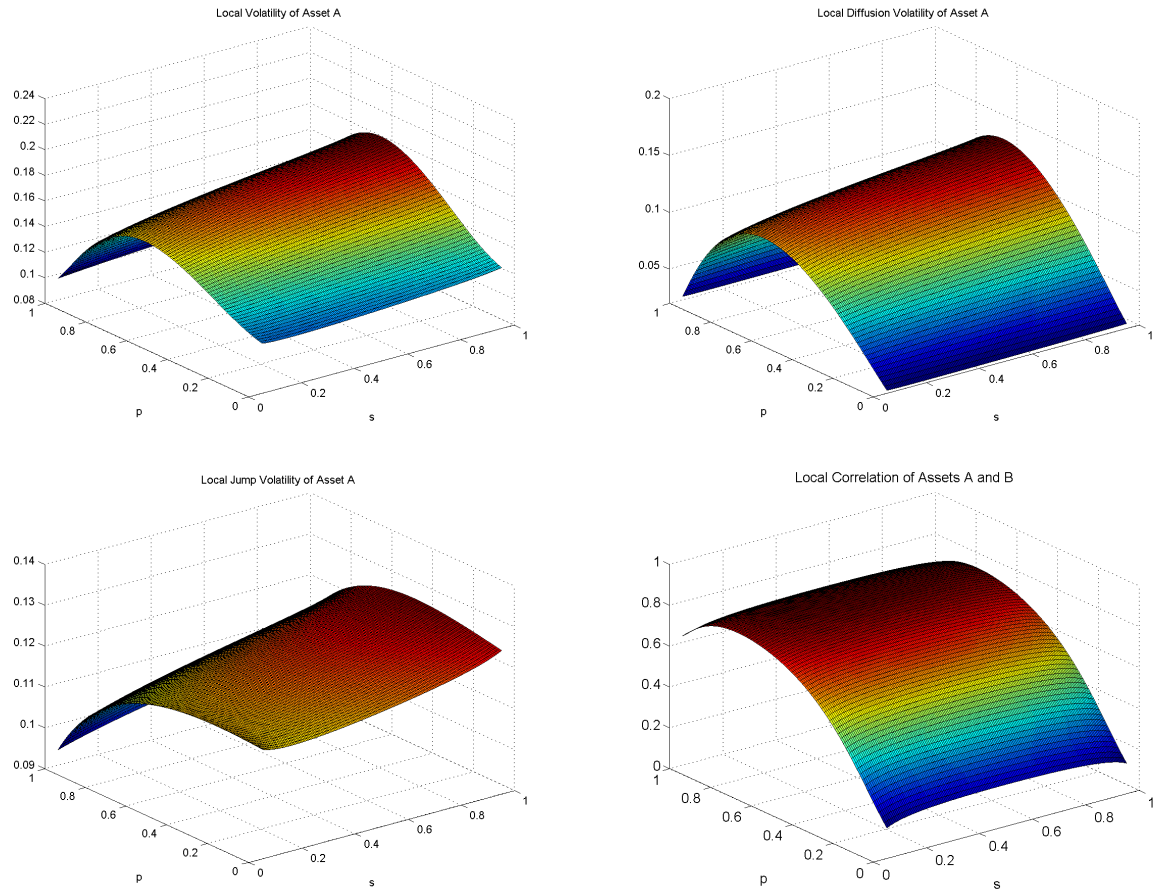

Figure 5: Local Volatilities and Correlations

The figure depicts a decomposition of the local return volatility of asset A (upper left picture) into the local volatility stemming from diffusive risk (upper right picture) and the local volatility stemming from jump risk (lower left picture). The lower right picture depicts the local return correlation of asset A and asset B. The independent variables in all graphs are the two state variables s_A and $\widehat{p}$. The results have been obtained using the benchmark calibration shown in the first column of Table 1.

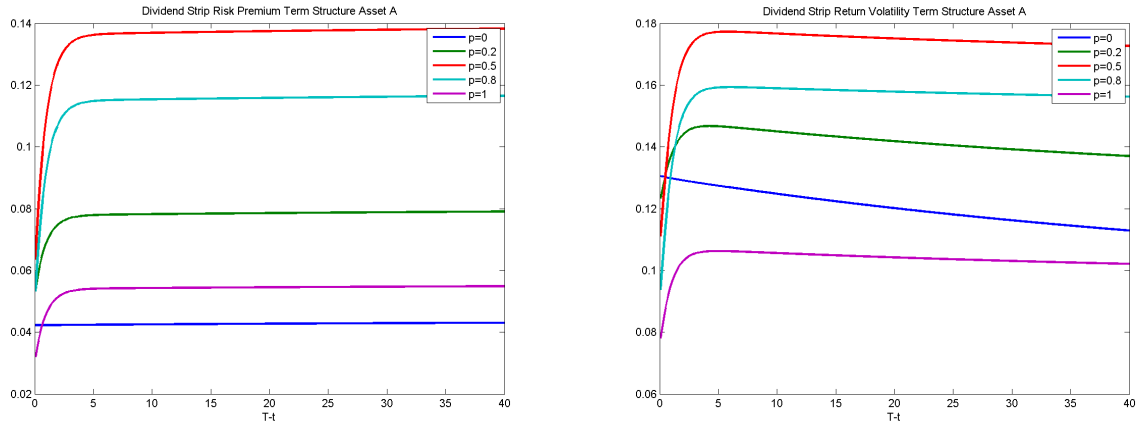

Figure 6: Term Structure of Equity for Asset A at $s_A = 0.5$ and for $\widehat{p} = 0, 0.2, 0.5, 0.8, 1$

The figure depicts the term structures of expected excess returns (left picture) and local return volatilities (right picture) of dividend strips on asset A. The term structures are shown for different $\widehat{p} = 0, 0.2, 0.5, 0.8, 1$ and a fixed output share of $s_A = 0.5$. The independent variable in both graphs is the time to maturity (in years) of the dividend strip. The results have been obtained using the benchmark calibration shown in the first column of Table 1.

CENTER OF EXCELLENCE SAFE

WORKING PAPER SERIES

Recent Issues

No. 33	Gabriele Camera, YiLi Chien	**Two Monetary Models with Alternating Markets**
No. 32	Gabriele Camera, Alessandro Gioffré	**Game-Theoretic Foundations of Monetary Equilibrium**
No. 31	Dirk Bursian, Sven Fürth	**Trust Me! I am a European Central Banker**
No. 30	Dirk Bursian, Markus Roth	**Optimal policy and Taylor rule cross-checking under parameter uncertainty**
No. 29	Iñaki Aldasoro, Ignazio Angeloni	**Input-Output-Based Measures of Systemic Importance**
No. 28	Nicole Branger, Holger Kraft, Christoph Meinerding	**Partial Information about Contagion Risk, Self-Exciting Processes and Portfolio Optimization**
No. 27	Tobias H. Tröger	**The Single Supervisory Mechanism – Panacea or Quack Banking Regulation?**
No. 26	Michael J. Brennan, Holger Kraft	**Financing Asset Growth**
No. 25	Holger Kraft, Alexander Schmidt	**Systemic Risk in the Financial Sector: What Can We Learn from Option Markets?**
No. 24	Andrej Gill, Nikolai Visnjic	**Performance Benefits of Tight Control**
No. 23	Andrej Gill, Nikolai Visnjic	**Insight Private Equity**
No. 22	Dirk Bursian, Alfons J. Weichenrieder, Jochen Zimmer	**Trust in Government and Fiscal Adjustments**
No. 21	Stefano Corradin, Reint Gropp, Harry Huizinga, Luc Laeven	**Who Invests in Home Equity to Exempt Wealth from Bankruptcy?**